Berenike Lisa Doler, BSc

# Metallation and Homo- or Heterocoupling Reactions of Diphenyltin dihydride

**MASTER'S THESIS**

to achieve the university degree of

Diplom-Ingenieurin

Master's degree programme:

Technical Chemistry

submitted to

**Graz University of Technology**

**Supervisor**

Assoc.Prof. Dipl.-Ing. Dr.techn. Roland Fischer

Institute of Inorganic Chemistry

Graz, April 2021

## AFFIDAVIT

I declare that I have authored this thesis independently, that I have not used other than the declared sources/resources, and that I have explicitly indicated all material which has been quoted either literally or by content from the sources used. The text document uploaded to TUGRAZonline is identical to the present master's thesis.

Date, Signature

To my family

# Danksagung

An dieser Stelle möchte ich mich bei all denjenigen bedanken, ohne die diese Abschlussarbeit nicht möglich gewesen wäre.

Zuallererst möchte ich mich sehr herzlich bei Roland Fischer bedanken, dass es mir überhaupt möglich war meine Masterarbeit in seiner Arbeitsgruppe schreiben zu können. Durch ihn habe ich die Chance erhalten mich mit einem äußerst spannenden und vielseitigen Thema auseinandersetzen zu dürfen. Die lehrreichen Tipps und die unzähligen motivierenden Gespräche sowie seine stets offene Bürotür sind entschiedene Gründe dafür, warum ich mich auf diesem Institut so wohl gefühlt habe und immer gerne dort gearbeitet habe.

Ich möchte mich auch bei meiner Schreibraumkollegin Beate Steller, für die sehr gute Zusammenarbeit, den Spaß im Labor und die lustigen und abwechslungsreichen Gespräche bedanken. Großer Dank gilt auch dem gesamten Institut für Anorganische Chemie, für den gegenseitigen Wissensaustauch und die gemeinsamen Kaffee- und Mittagspausen, die mir immer Freude und Motivation geschenkt haben.

Besonders großer Dank gebührt meinem Freund Samuel, der mit seiner fröhlichen, herzlichen Art ständig für mich da war und mich immer zum Lachen gebracht hat, wenn ich es am meisten gebraucht habe. Ich bin unendlich dankbar für die vielen schönen und lustigen Momente die wir bisher gemeinsam verbracht haben.

Der wohl größte Dank gilt meinen Eltern sowie meiner gesamten Familie, die mir in den letzten Jahren stets zur Seite standen und mich in meinen Entscheidungen immer unterstützt und bestärkt haben. Durch ihre finanzielle Unterstützung aber vor allem durch ihren emotionalen Rückhalt ist das Verfassen dieser Arbeit überhaupt möglich. Ich möchte mich auch bei meiner großen Schwester, meiner besten Freundin, Carina bedanken. Die für mich rund um die Uhr da war und stets ein offenes Ohr hatte. Sie ist für mich der Mensch auf den ich immer zählen kann.

# 1 Abstract

This master thesis presents the investigation of metalation reactions of diphenyltin dihydride [$Ph_2SnH_2$], by using alkaline metal derivates like methyllithium, *n*-Buthyllithium and lithium-bis(trimethylsilyl)amide or alkaline metals like lithium, sodium, rubidium or cesium. The main goal in particular, was the isolation of monometallated monomeric and dimeric species by heteronuclear NMR and X-Ray crystallography in order to understand their following coupling reactions and the formation of anionic tin oligomers. Furthermore, to improve the synthesis and to get an idea of how the metallated tin oligomers grow, different reaction conditions were tested, like the change of solvent, temperature or quantity of the reagents. Isolated molecular compounds are characterized by state-of-the-art methods including heteronuclear NMR, UV/VIS spectroscopy as well as X-Ray crystallography.

# 2 Kurzfassung

Diese Masterarbeit befasst sich mit der Untersuchung von Metallierungsreaktionen von Diphenylzinndihydrid [$Ph_2SnH_2$], durch Verwendung von Alkalimetallderivaten wie zum Beispiel Methyllithium, *n*-Buthyllithium und Lithium-Bis (trimethylsilyl) amid oder Alkalimetallen wie Lithium, Natrium, Rubidium oder Cäsium. Hauptziel war die Isolierung monometallierter monomerer und dimerer Spezies, charakterisiert durch heteronukleare NMR Spektroskopie und Röntgenkristallographie, um die folgenden Kupplungsreaktionen und die Bildung anionischer Zinn-Oligomere besser zu verstehen. Um die Synthese zu verbessern und eine Vorstellung davon zu bekommen, wie die metallierten Zinn Oligomere wachsen, wurden verschiedene Reaktionsbedingungen, wie die Änderung des Lösungsmittels, der Temperatur oder der Menge der Reagenzien, getestet. Die isolierten molekularen Verbindungen wurden mittels moderner Analysemethoden, darunter heteronuklearer NMR Spektroskopie, UV/VIS-Spektroskopie sowie Einkristallstrukturanalyse, untersucht.

# Contents

# 3 Literature

## 3.1 Organometallic hydrides of Group 14 elements

Group 14 elements play an important role in various metathesis reactions. Especially organotin hydrides, like for example tributyltin hydride, are extremely imperative reducing agents in organic synthesis. The first stable hydrides detected had been restricted to derivates in tetravalent state.[1] However, the situation changed with the work of Power *et al*. It was also shown that a divalent tin(II)hydride $(Ar^*SnH)_2$ could be prepared by using the sterically demanding Ar* ligand (Ar*=$C_6H_3$-2,6-($C_6H_2$-2,6-*i*$Pr_2$)$_2$).[2] Bis(aryl) tetrylenes, $[(Ar)_2E]$ (E = Ge, Sn; Ar = $^{Mes}$Terph or $^{Dipp}$Terph), ($^{Mes}$Terph = $C_6H_3$-2,6-($C_6H_2$-2,4,6-*t*-$Bu_3$)$_2$; $^{Dipp}$Terph = $C_6H_3$-2,6-($C_6H_3$-2,6-*i*$Pr_2$)$_2$) can react with $H_2$ under the formation of either $Sn^{II}$ or $Ge^{IV}$ hydride species via an oxidative addition, in the case of germanium$^{IV}$ and via reductive elimination at $Sn^{II}$ compounds (Scheme 3.1).[3]

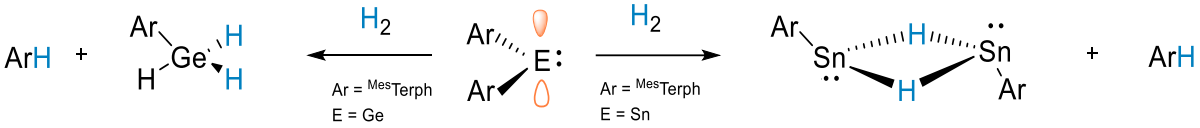


**Scheme 3.1** Reactions of bis(aryl)tetrylenes with dihydrogen leading to oxidative addition [3]

Dihydrides of group 14 elements in low oxidation state (+II) are highly reactive. Therefore $EH_2$ (E = Si, Ge, Sn, Pb) are of high interest, due to their potential role as intermediates in semiconductor synthesis. As reported by Rivard *et al.* parent $GeH_2$ and $SnH_2$ complexes can be stabilized by using $BH_3$ as acceptor and NHC (N-heterocyclic carbene) as a donor.[4] According to that research a likewise strategy was employed by Robinson *et al.* to synthesize Si(II) hydride.[5]

## 3.2 The Sn-H bond

Tin, with an average Sn-H bond energy of only 253 kJ $mol^{-1}$, represents a rather weak bond to hydrogen in comparison to the other group 14 metals. The Ge-H bond is quite robust, with a bonding energy of 260 kJ $mol^{-1}$, although weaker than the Si-H bond (322 kJ $mol^{-1}$). Stannane ($SnH_4$) itself undergoes rapid decomposition at room temperature and oxygen under the formation of elemental tin and hydrogen. The high sensitivity of tin towards temperatures can be lowered by the substitution of a hydrogen atom with sterically more demanding ligands.

Tin-hydrides $R_nSnH_{4-n}$ are stable against moisture however, they are thermolabile and quickly react with oxygen to form the corresponding hydroxides or oxides. With increasing number of organic ligands "R" or the increasing sterically hindrance of the ligands also the tolerance of tin-hydrides $R_nSnH_{4-n}$ towards heat and oxygen increases.[6]

Preparation methods yielding organotin hydrides were firstly revealed in 1922 by Kraus and Geer who successfully synthesized trimethyltin hydride.[7] This working group used sodium triorganostannides, $R_3SnNa$, with ammonium chloride in liquid ammonia (Scheme 3.2).

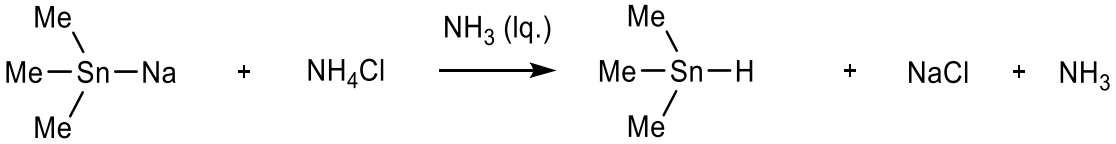


**Scheme 3.2** Equation of the preparation of trimethylstannane in a liquid ammonia solution[7]

Later Finholt *et al.* developed a more convenient approach. To synthesize organic derivatives, they used the corresponding chloride and lithium aluminium hydride ($LiAlH_4$) as starting material. By using this method, the working group was able to generate methyltin trihydride, dimethyltin dihydride and trimethyltin hydride.[8] Even today this synthetic procedure represents a convenient strategy for the formation of mono-, di- and trihydrido organotin compounds ($R_3SnH$, $R_2SnH_2$, $RSnH_3$) in high purity and yield.[9]

## 3.3 Reactivity and application of tin hydrides

Several factors have significant impact on the chemical reactivity of organotin hydrides. One main factor is the sterically hindrance of the ligands. In Scheme 3.3. the drop in reactivity of tin hydrides is demonstrated. The more sterically, more demanding and shielding the ligands become the less reactive is the resulting tin hydride.

**Scheme 3.3** Reactivity of tin hydrides depending on their ligands

However, not only the ligands have a tremendous effect on the reactivity also the choice of the right solvent (for example polar solvents promotes heterolytic reactions) and the reaction conditions show an influence on the reactivity of tin hydrides.[10,11]

Under the abstraction of the hydrogen atom, tin hydrides can undergo the following reactions types:

a) reaction with a nucleophile

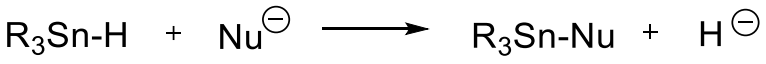

b) reaction with a base

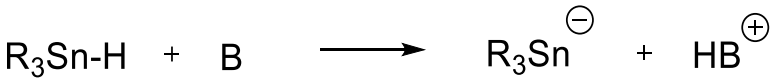

c) reaction with an electrophile

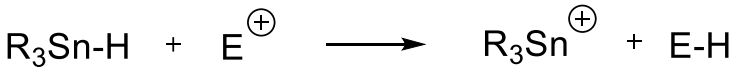

d) reaction with a radical

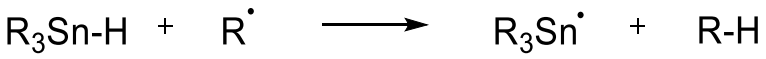

e) reductive elimination/ oxidative addition

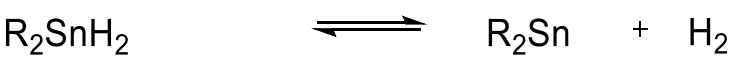

f) Insertion of Sn-H bond

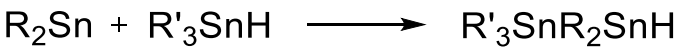

### 3.3.1 Hydrostannolysis and Hydrostannation

The tin-hydrogen bond, can be homolytically cleaved, because it shows a non-ionic behaviour. Tin compounds are widely used in radical reactions of organic synthesis as reducing agents. However, due to their labile nature they found wide application in organic synthetic chemistry like hydrostannolysis and hydrostannation (see Scheme 3.4). For that kind of reactions, specifically, $Bu_3SnH$ (tributyltin hydride) is widely used due to its low price, lower toxicity, reactivity and ease of handling. The stannane intermediate easily can decompose in the presence of a proton donor to a reduced carbonyl compound.[12]

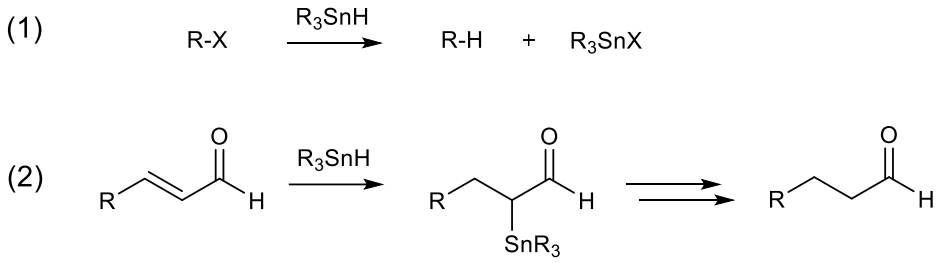


**Scheme 3.4** (1) Hydrostannolysis (2) Hydrostannation[6]

### 3.3.2 Sn-Sn bonds

The bond dissociation energy of Sn-Sn bonds in diatomic molecules is only low, especially when it is compared with the bond dissociation energy of C-C. This indicates that the Sn-Sn bond is quite unstable. However, on the other hand the bond dissociation energy rises when methyl, or even better ethyl groups are coordinated on Sn. Then the bond dissociation energy is very close to the value of two coordinated methyl groups. All bond dissociation energies discussed can be seen below in Figure 3.1. These data represent that the stability of polystannanes is considerably influenced by their side groups R. With sterically demanding ligands like alkyl or aryl groups the thermally stability of polystannanes can be increased and therefor the compound can be easily handled at room temperature without problems.[13]

| | | |
|---|---|---|
| **Sn – Sn** | 187 kJ mol-1 | (1) |
| **C – C** | 618 kJ $mol^{-1}$ | (2) |
| **$Me_3Sn – SnMe_3$** | 290-300 kJ $mol^{-1}$ | (3) |
| **$Et_3Sn – SnEt_3$** | 354 kJ $mol^{-1}$ | (4) |
| **$CH_3 – CH_3$** | 377 kJ $mol^{-1}$ | (5) |

**Figure 3.1** Bond dissociation energy of Sn-Sn compounds and C-C in comparison

### 3.3.3 Metalation of Sn-Sn bonds

Metalation reactions of tinhydrides can be carried out with strong bases like lithium amides, $^{n}$BuLi, methyllithium, Grignard reagents or alkali metal hydrides as metalating agents.

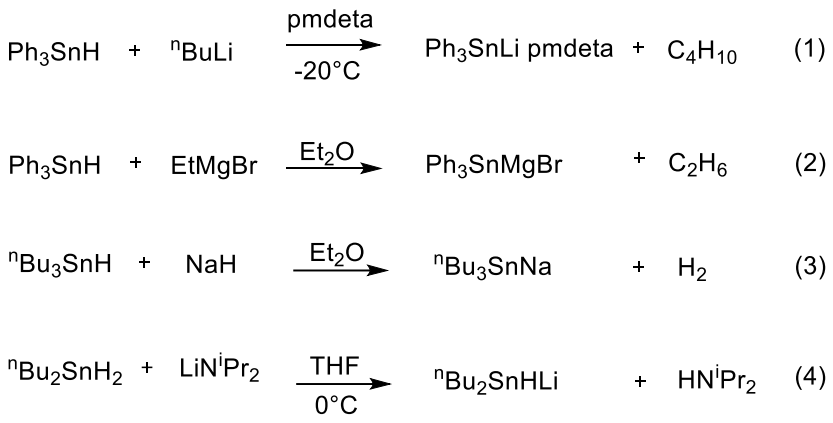


**Figure 3.2** Metalation reactions of organotinhydrides with strong bases

A common side reaction of organotin hydrides is the formation of Sn-Sn bonds. This reactivity was also investigated by the working group of Reimann in 1978. A reaction was executed twice, under otherwise identical conditions, where only the solvent was changed from THF to diethyl ether (see Scheme 3.5). The experiment shows, that if the reaction is carried out in tetrahydrofuran (THF) as solvent, the trimethylstannyl lithium species is gained. However, using $Et_2O$ as solvent Sn-Sn bonds form and hexamethyldistannane could be detected.

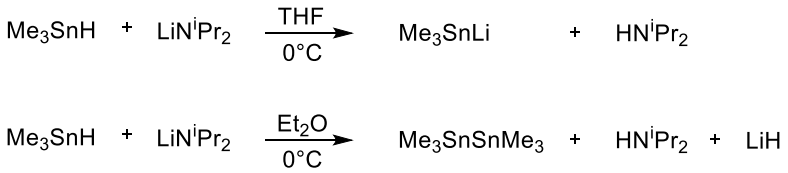


**Scheme 3.5** Reaction of $Me_3SnH$ with lithium diisopropyl amide (LDA) in different solvents[14]

In their research, Podesta *et al*. present the effect of sterically demanding substituents on the reactivity of tin hydrides. In comparison are trineophyl tin hydride $Nph_3SnH$ (Nph = Neophyl = $-CH_2-CMe_2Ph$) and the methyldineophyl tin hydride $MeNph_2SnH$. The reaction route with methyldineophyl, the less sterically demanding group, and NaH in dimethyl sulfoxide (DMSO) yields to the Sn-Na bond. Whereas the reaction with trineophyl tin hydride and NaH in DMSO, leads to the Sn-Sn coupling product.[15]

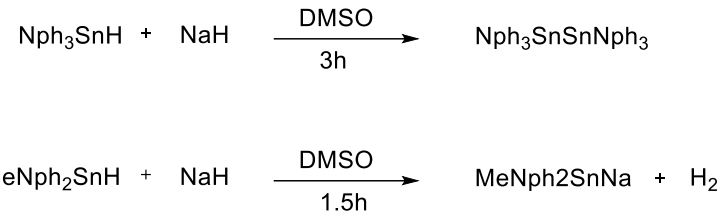


**Scheme 3.6** Reactions of $Nph_3SnH$ or $MeNph_2SnH$ (Nph= $-CH_2-CMe_2Ph$) with NaH in DMSO[15]

The choice of the right solvent is also important in metalation reactions, as it could be seen in Scheme 3.5. The reactivity of metalation agents depends on their solubility. On the example of two frequently used metalating agents like methyllithium and *n*-Butyllithium. Both are highly reactive, but in terms of different solubility and structure they vary. In this section the structure in solid state as well as in dissolved state in order to their reactivity is reported.

### 3.3.3.1 Methyllithium

MeLi is known as a very powerful nucleophile and strong basic. In solid state four $CH_3Li$ molecules combine to a tetrameric subunit. Four lithium atoms and four methyl groups occupy the corners of two interpenetrating tetrahedra, like in the figure below.[16]

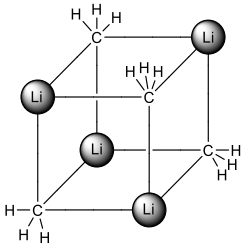


**Figure 3.3** Tetrameric structure of cubic arranged $(MeLi)_4$

In the tetrameric structure every Li-atom has close contacts with three charged carbons.[17] The fourth side is close to electron-rich CH bonds of a other cluster. In the presence of unpolar solvents MeLi cannot be dissolved because of polymer-formation. In contrast with ether, like THF (tetrahydrofuran), it is readily soluble. The fourth valence of Li-atoms are saturated by free electron pairs from the ether.

### 3.3.3.2 *n*-Buthyllithium

The structure of *n*-BuLi in solid state is a hexamer of eight Li-atoms octahedral arranged (figure 3.4). *n*-BuLi solvated in ether, like THF (tetrahydrofuran), receives more attention because of an observed increase in reactivity. In diethyl ether and THF, *n*-BuLi exists in a tetrameric structure.[18]

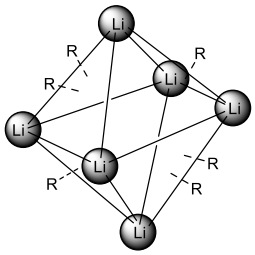


**Figure 3.4** Hexameric structure of octahedral arranged $(n\text{-BuLi})_6$ (R= $C_4H_9$)[19]

## 3.4 Polystannanes

### 3.4.1 Tin-Tin Bond formation, Wurtz coupling

As shown in the previous section, tin hydrides can also form tin-tin bonds. Two types of reactions exist:

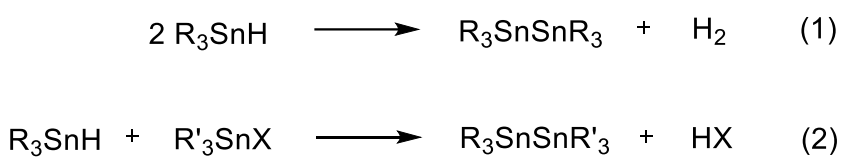


**Scheme 3.7** Reaction of tin hydrides to form Sn-Sn bonds[11]

Reaction (1) occurs in the presence of a Lewis base (for example pyridine) or might be induced by a transition metal catalyst like $Rh^{I}$. The mechanism of these reactions is not fully understood so far, but seems to involve anions $R_3Sn$ in the case of strong bases. However, the base-induced elimination of hydrogen from $R_2SnXH$ has been shown to involve a radical chain mechanism, which will be discussed in section 3.4.2 in more detail.

While monofunctional stannanes, $R_3SnH$, produce distannanes in coupling reactions, difunctional starting materials, e.g. diorganotin dihydrides $R_2SnH_2$, can employ in the preparation of cyclic compounds, linear oligomers or polymers. Besides catalytic reactions of $R_2SnH_2$, also other methods have been applied like the Wurtz coupling. In this type of reaction an alkali metal (typically Na but also Li, K, Rb, Cs) is dissolved in solvents, like for example toluene and with $R_2SnCl_2$ it reacts to finally obtain poly(dialkylstannane). Until today the Wurtz coupling is the conventional reaction method to synthesize poly(dialkylstannane) even though only low yields and many byproducts (cyclic oligomers) are obtained. In the Wurtz coupling reaction the alkali metal acts as reducing agent, while the electrons might be alternatively directly induced by electrolysis.[13]

Another way of synthesizing polystannanes is electrochemical synthesis. In that kind of reaction dichlorodiorganostannanes, $R_2SnCl_2$ are applied to create poly(dialkylstannanes) by electrochemical reduction.

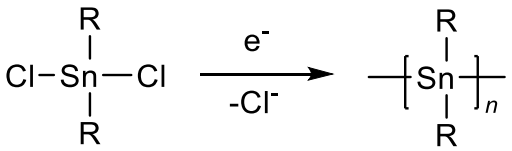


**Scheme 3.8** Electrochemical synthesis of dichlorodiorganostannanes

### 3.4.2 Dehydrogenative coupling catalysed by an amine base

In the early 1960s Neuman *et al.*[20] described the addition of a nitrogen base to a tin hydride solution yielding a Sn-Sn bond. Those studies show that the dehydrogenation process is intermolecular and takes place at the ends of a growing chain H-($R_2$Sn)-H and disfavours the assumption that free $R_2$Sn groups are involved in that reaction. The working group of Davies[21] later successfully developed this field further. As mentioned before the reaction mechanism can act via a radical chain mechanism. The radical chain mechanism occurs through a SH2 (homolytical substitution) reaction between the tin radical and the tin hydrogen bond forming a new Sn-Sn bond and a hydrogen radical. This hydrogen radical would then be expected to abstract another hydrogen from the Sn-H bond forming $H_2$.

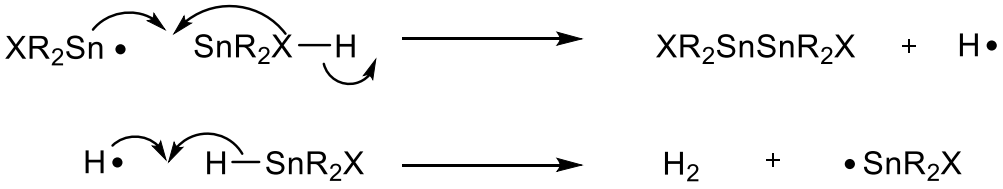


**Scheme 3.9** Radical chain mechanism of amine based catalysed reactions[21]

In 2015 Sindlinger *et al.* published the dehydrogenative coupling reaction of organotin trihydride Ar*$SnH_3$ (Ar* = 2,6-$trip_2(C_6H_3)$, trip = 2,4,6-triisopropylphenyl). They successfully observed the dehydro-coupling product diorganodistannane Ar*$H_2$Sn$SnH_2$Ar* by using catalytic amounts of amine base like DMAP (4-dimethylaminopyridine), pyridine and TMEDA (tetramethylethyle diamine). The reaction scheme (3.10) is shown below.[22] In this case, however, no radical pathway seems to be operative but rather involves the intermediate formation of a base stabilized heterosubstituted stannylene RHSn.

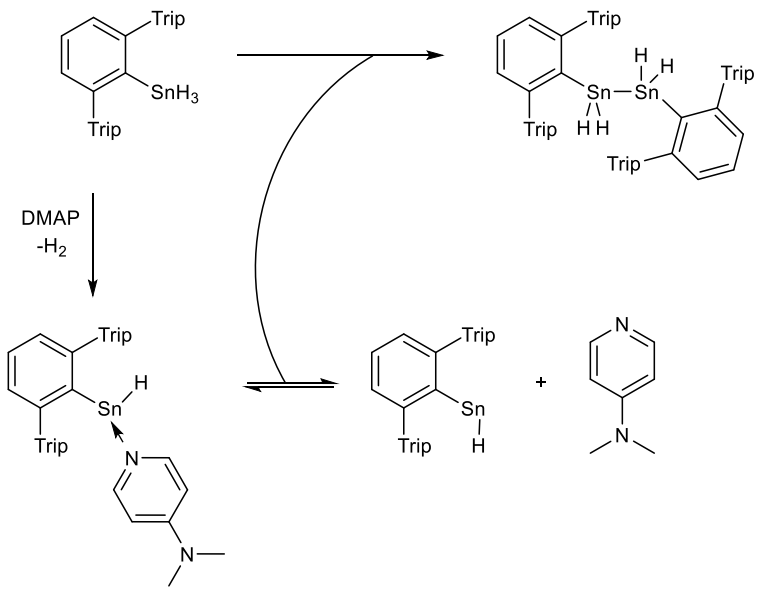


**Scheme 3.10** Dehydrogenation of Ar*$SnH_3$ using DMAP as amine base[22]

### 3.4.3 Dehydrogenative coupling catalysed by a transition metal

Metal catalysed dehydrogenative coupling of tin hydrides forming distannanes was established with Pd(II) complexes for the first time. However until today a large number of transition metals including: Au(II), Ru(II), Y(III), Ti(IV), Zr(IV), Hf(IV), Vr(0), Mn(0), W(0), Rh (III) have been confirmed to effectively catalyse dehydrogenative coupling of tin hydrides as well.

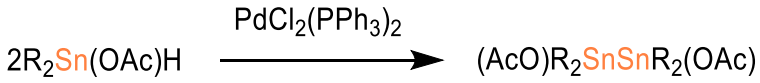


**Scheme 3.11** Reaction example for dehydrogenative coupling catalysed by a Pd(II) complex

The mechanism of the reaction, is usually thought to involve the formation of an M-$SnR_3$ complex which reacts directly, or via $HM(SnR_3)_2$ to give MH and $R_3SnSnR_3$.[11]

However, that is not valid for all metal catalysed dehydrogenated couplings. Like the work of Tilley *et al*.[23] in 2001 showed, the reaction of Cp*CpHfClH (Cp*= $Me_5C_5$) with $Mes_2SnH_2$ is believed to proceed *via* the elimination of stannylene $Mes_2Sn$**:** from Cp*CpHfCl-$SnHMes_2$, followed by insertion of $Mes_2Sn$**:** into the Sn-H bond of $Mes_2SnH_2$ (see Scheme 3.12).[11]

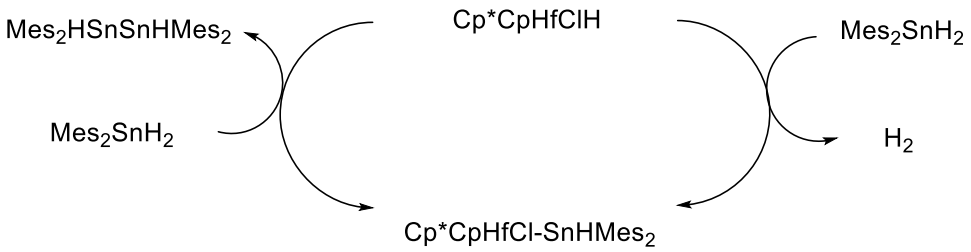


**Scheme 3.12** Reaction scheme of $Mes_2SnH_2$ and Cp*CpHfClH[23]

Unfortunately, this experiment yielded in a mixture of cyclic-oligomers and products with low molar mass.

The mentioned examples of catalytic dehydrogenative coupling reactions catalysed by transition metals typically have low yields and a high formation of byproducts like cyclic oligomers. However, Choffat *et al.* revealed a synthetic route where linear polystannanes can be synthesized in high yield (~100%) while the formation of low molecular weight oligomers is supressed.

In this type of reaction the catalyst species used is the Wilkinson catalyst $[RhCl(PPh_3)_3]$ which reacts with $Bu_2SnH_2$ under formation of hydrogen to *poly(dibutylstannane)*. The success might be associated with the two stable oxidation states of rhodium (I & III) which come along with a change in the coordination geometry from square planar ($d^8$) configuration of $Rh^I$ to octahedral ($d^6$) configuration of $Rh^{III}$. This probably prefers the catalytic process on oxidative addition and reductive elimination.[24]

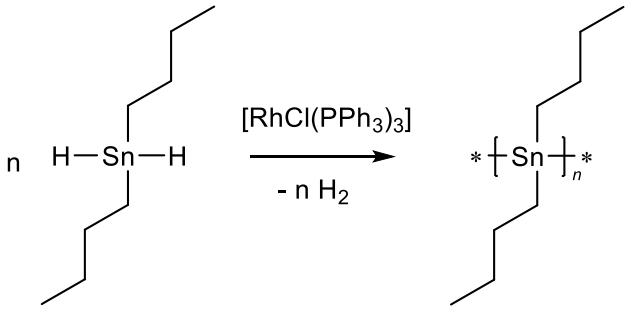


**Scheme 3.13** Synthesis of poly(dibutylstannane)[24]

The development of dehydropolymerization can be followed quantitatively by $^1H$ NMR spectroscopy, the evolution of hydrogen revealed during the reaction, or qualitatively by infrared spectroscopy.[13]

### 3.4.4 Structure and Properties of Polystannanes

Polystannanes $(SnR_2)_n$ describe a class of inorganic polymers as their backbone consists of covalently bound tin atoms. The Sn-Sn bond, with a length of 2.85 Å is much longer than Si-Si (2.35 Å) or Ge-Ge (2.50 Å) bonds, but the barrier of rotation for Sn-Sn is smaller than in Si-Si or Ge-Ge analogues. Due to that fact the rotational motion about the Sn-Sn bonds is free.[25] It seems yet that polystannanes are the only linear polymers which are established only by metal-metal bonds. The usual chemical structure of polystannanes can be seen in Figure 3.5. The fact that tin atoms are arranged in line is possible due to the four atoms bonded to Sn. This leads to a tetrahedron "zig-zag" structure. A considerable feature of this polymers is the delocalization of electrons along the polymer backbone, known as σ-delocalization, which will be discussed in section 3.4.5 in more detail. A helical structure was proposed by Tilley based on powder XRD data.

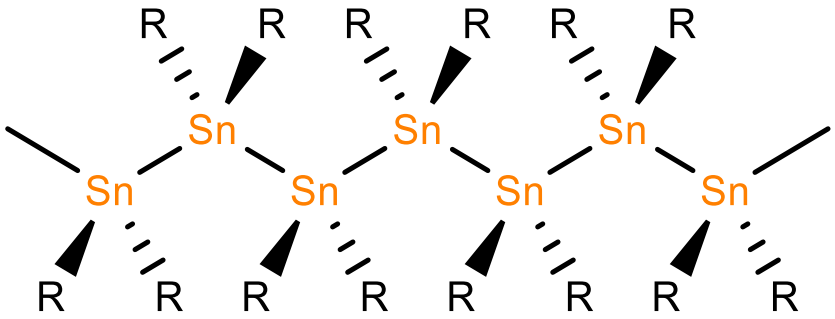


**Figure 3.5** Schematic representation of a sequence of polystannanes[13]

A remarkable drawback of polystannanes is their limited stability against light, especially in solution. Under the exposure of light, the polymer in solution degrades very fast. When degradation starts, cyclic oligomers with five or more tin atoms, as well as byproducts, are formed. It is believed that dissolved polystannanes undergo a light-induced homolytical cleavage of the Sn-Sn bond generating two tin radicals, which further undergo the degradation processes, like the unzipping process. Whereas the formed radicals initiate a running release until the polymer chain is completely degraded. It is worth noting that the degradation tendency is dependent on the grade of solubility. The more soluble the polystannanes are, the higher is the degree of degradation under the action of light.[13] A schematic representation of the polystannane degradation can be seen in Figure 3.6.

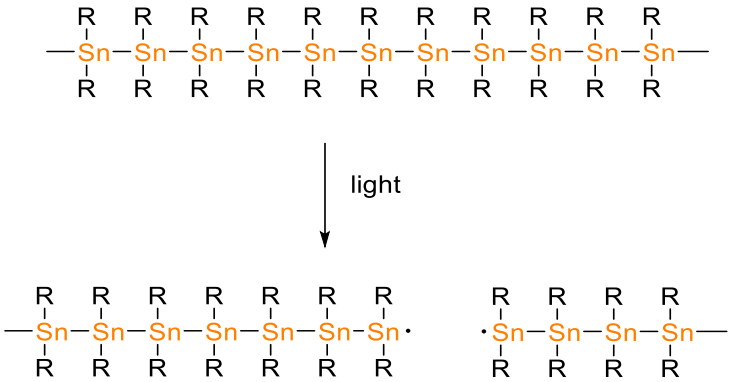


**Figure 3.6** Schematic representation of polystannane degradation under the action of light[13]

### 3.4.5 σ-delocalization

Even though tin is a group 4 element like carbon there are many differences in their chemistry and properties. A considerable difference between tin and carbon polymers is the delocalization of σ-electrons in polystannanes. This effect of delocalization of σ-electrons was first found for polymers with a silicon backbone by West *et al*. in 1986.[26] Later it could be demonstrated, that the overlap of atomic orbitals is more pronounced for backbone of tin atoms than for Ge or Si atoms corresponding to a lower band gap energy, by exchanging integrals between the ground state and the first excited state of adjacent atoms. An improvement of the Hückel molecular orbital theory, called “Sandorfy model C approximation” was applied. This shows that $sp^3$ hybrid orbitals are responsible for bond formation in the polymer backbone with two resonance integrals, a strong vicinal interaction of two overlapping $sp^3$ orbitals of neighbouring atoms and a weaker geminal interaction of $sp^3$ orbitals at the same atom. The ration between these two resonance integrals describe the degree of delocalization of the molecular orbitals. The extent of σ-conjugation depends on the conformation of polystannanes backbone which is expected to be mostly found in the trans-planar structure.

If aromatic side groups, like a phenyl for example, are present in a polystannanes also σ-π conjugation between the aryl group and the polystannanes backbone occur in the compound (see Figure 3.7).[10]

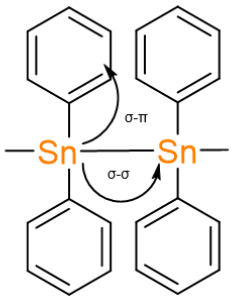


**Figure 3.7** Illustration of a σ-σ bond conjugation and an σ-π conjugation[10]

Delocalization of electrons from π-conjugation is more common than the delocalization of σ-electrons in chemistry. However, it is known that typical effects of π-conjugation like electric semi conductivity and a red shift in optical absorption with an increasing number of Sn-atoms also arise when σ-conjugation occurs.[10,13]

In 2016 Caseri showed, that the absorption maximum in UV-VIS spectroscopy of dialkylstannanes (including phenyl-terminated groups), occurs typically in the region of 370-400 nm. By increasing number of Sn atoms, the $\lambda_{max}$ increases, as a result of σ-delocalization. For a dimer, like poly(dibutylstannane) the $\lambda_{max}$ is below 240 nm. This term increases until a plateau value of 380 nm, at about 40 tin atoms.

Polystannanes with substituted phenyl groups (shown in Figure 3.8) commonly exhibit an absorption maximum between 420 nm and 470 nm and with disubstituted $[Sn(2,4\text{-}C_3H_6EtOBu)_2]_n$ wavelength at 506 nm are observed. Poly(diarylstannane)s which include electron withdrawing groups like $CF_3$ decrease the σ- electron conjugation. As a result the absorption maximum is shifted to lower wavelengths at around 330 nm.

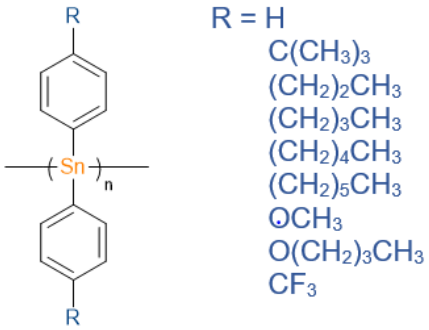


**Figure 3.8** Aromatic polystannanes with different substituents R|[13]

The change of the substituent R could also be detected by NMR spectroscopy by Caseri. For (-$SnR_2$)- compounds NMR spectroscopy turns out to be a powerful tool. Using $^{119}$Sn NMR spectroscopy a change of the chemical shift depending on the substituent R of an $(SnR_2)_n$ group can be quantitatively determined. In terms of linear poly(dialkylstannane)s including phenyl-terminated polystannanes, like shown in Figure 3.8, chem. shifts at -189 ppm or -195 ppm. At (R = Et) shifts at -172 ppm are expected and cyclic oligomers around -200 ppm and -208 pm.[13]

# 4 Result and Discussion

## 4.1 Diaryltindichloride and Diaryltindihydride

The most important starting material for any further synthesis routines during the term of this master thesis, is **$Ph_2SnH_2$**. $Ph_2SnH_2$ was prepared following a two reaction step route, according to Scheme 4.1.

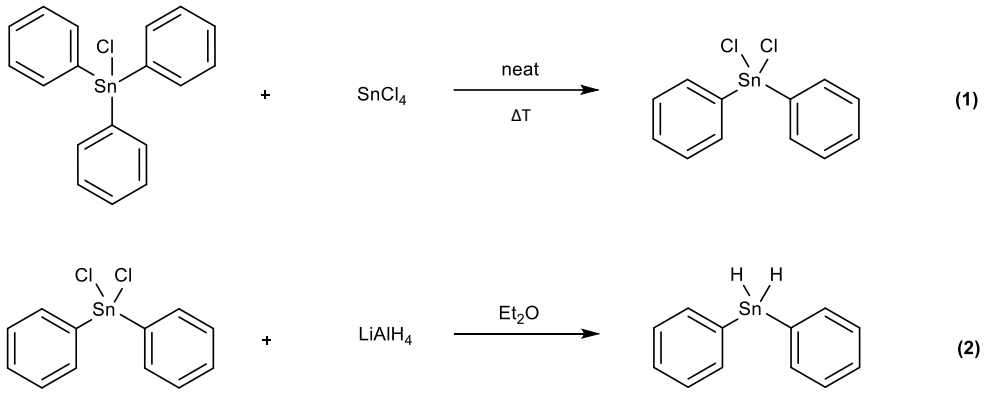


**Scheme 4.1** Reaction route for the synthesis of $Ph_2SnH_2$

For the first step **(1)**, the synthesis of diaryltin dihalide ($Ph_2SnCl_2$), the common routine *via* Kozeshkov redistribution reaction was elected based on phenyl group transfer between commercially available $Ph_3SnCl$ and $SnCl_4$, c.f. Scheme 4.1 (1). After recrystallization from heptane, yields in the area of 90% were realized.[9] [10] The product was characterised by $^{1}H$ and $^{119}Sn$ NMR spectroscopy. In order to obtain the diphenyltin dihydride species a similar synthesis route according to the literature was executed.[8] However, unlike to the synthesis method of that working groups, who carried out the reaction at -30°C with an excess on $LiAlH_4$, the reaction temperature was raised to 0°C and an optimal stochiometric ratio of educt and reducing agent (1.0:0.8 eq.) was improved. The reduction of the amount of $LiAlH_4$ leads to a higher yield due to less significant side reactions.[10]

### 4.1.1 Metallation of $Ph_2SnH_2$ by organolithium reagents

Reports of Caseri *et al*. propose the formation of tetraphenyldistannide $(Ph_4Sn_2)^{2-}{}_2$ and diphenylstannide ($HPh_2Sn^-$) during the reaction of diphenyltindihydride exposed to sodium in liquid ammonia.[27] Although the authors imply the formation of the hydride substituted anion $HPh_2Sn^-$, from NMR spectroscopic data, this key intermediate has never been isolated in substance. In order to proof this results the intermediate, diphenyl tin monoanion, was tried to be isolated and analysed by NMR as well as X-ray spectroscopy. The study of this intermediate is a very important and critical step for the explanation of any further steps to organostannanes.

As starting material for further reaction routes $Ph_2SnH_2$ was used and exposed to different deprotonation agents, temperatures and solvents. All reactions were carried out in a nitrogen flushed Glovebox UNILAB supplied by M.Braun.

1.) Deprotonation agent: **Methyllithium;** Solvent: **THF**

In order to assess the reactivity of diphenytin dihydride towards strong deprotonating agents (i.e. strong Brønsted bases), the reaction between $Ph_2SnH_2$ and methyllithium was investigated. In initial experiments, $Ph_2SnH_2$ was reacted with one equivalent of MeLi in THF with and without addition of 12cr4 as a sequestering agent for the lithium cation.

The two reactions were carried out following the same protocol. First diphenyltin dihydride was dissolved in 10 mL THF, then MeLi was added dropwise via canula. In a final step (if mentioned) 12cr4 was added, to strongly coordinate the lithium cation.

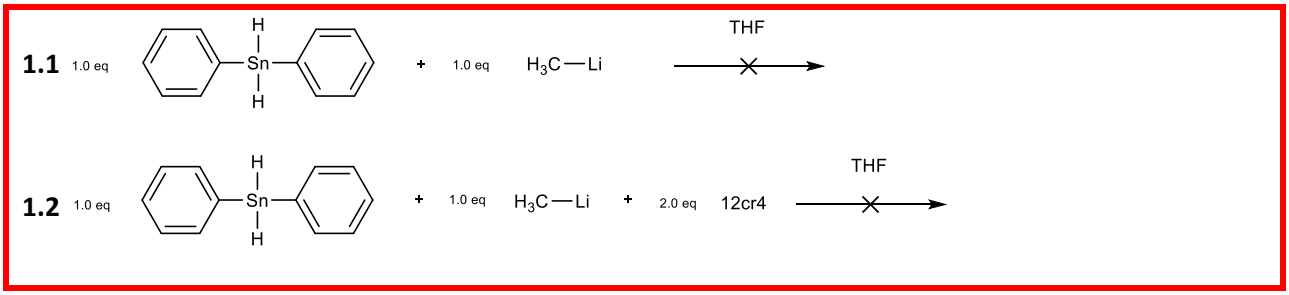


**Scheme 4.2** Reactions **(1.1)(1.2)** of $Ph_2SnH_2$ with MeLi in THF

In the first two experiments it can be seen that if a ratio of 1:1 between $Ph_2SnH_2$ to MeLi is used, no reaction takes place, even though at reaction **(1.2)** 12cr4 was used. In both cases the solution quickly gets cloudy and after a day a black precipitate is formed (elemental tin). However, in both cases no traceable molecular product is formed, while only decomposition products are observed.

In reactions **(1.3)** and **(1.4),** $Ph_2SnH_2$ and MeLi with a ratio of 1:0.1 **(1.3)** or 3:1 **(1.4)** were used. In both reactions following the 1:1 stoichiometry no traceable reaction products were detected spectroscopically. Hence, when THF is used as solvent, an excess of $Ph_2SnH_2$ was applied, to obtain isolable reaction products. Both reactions were carried out at room temperature and immediately yielded clear yellow solutions.

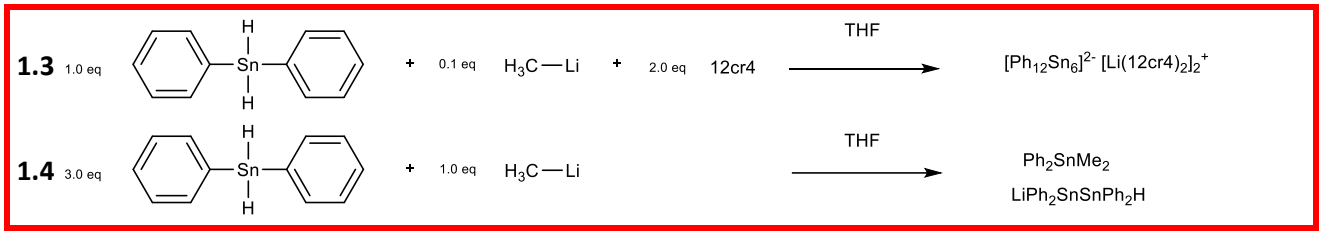


**Scheme 4.3** Reactions **(1.3)(1.4)** of $Ph_2SnH_2$ with MeLi in THF

Reaction **(1.3)** lead to formation of $[Ph_{12}Sn_6]^{2-}$ $[Li(12cr4)_2]_2^+$, as evidenced by $^{119}$Sn-NMR-spectroscopy and confirmed by single crystal X-ray diffraction structure analysis.

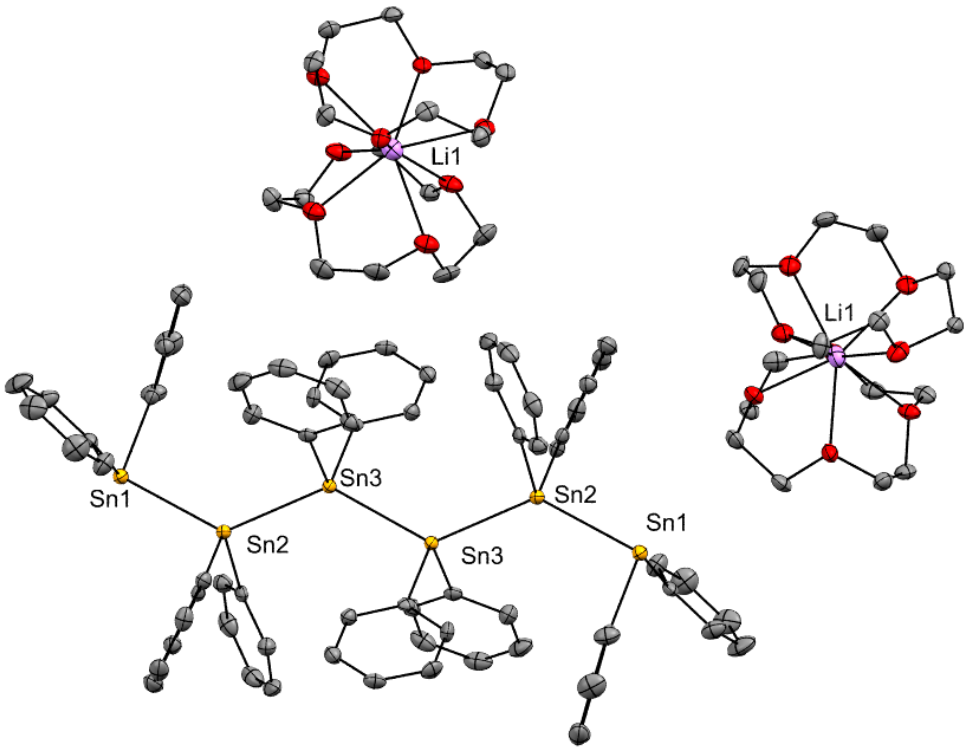


**Figure 4.1** Molecular structure of **$[Ph_{12}Sn_6]^{2-}$ $[Li(12cr4)_2]_2^+$**Hydrogens are omitted for clarity. Ellipsoids shown at a probability of 30%. Selected bond lengths [Å] and angles [°]: Sn1-Sn2 2.8818(3), Sn1-C1 2.224(3), Sn1-C7 2.210(3), Sn2-Sn3 2.8363(3), Sn2-C13 2.193(3), Sn2-C19 2.178(3), Sn3-C25 2.165(3), Sn3-C31 2.170(3), Sn3-Sn3 2.8284(3), Sn1-Sn2 2.8818(3), Sn1-C1 2.224(3), Sn1-C7 2.210(3), Sn2-Sn3 2.8363(3), Sn2-C13 2.193(3), Sn2-C19 2.178(3), Sn3-C25 2.165(3), Sn3-C31 2.170(3); Sn2-Sn1-C1 98.83(8), Sn2-Sn1-C7 104.03(8), C1-Sn1-C7 98.8(1), Sn1-Sn2-Sn3 131.08(1), Sn1-Sn2-C13 107.40(8), Sn1-Sn2-C19 102.66(8), Sn3-Sn2-C13 104.44(8), Sn3-Sn2-C19 108.44(8), C13-Sn2-C19 98.2(1), Sn2-Sn3-C25 105.09(8), Sn2-Sn3-C31 105.12(8), Sn2-Sn3-Sn3 129.79(1), C25-Sn3-C31 105.4(1), C25-Sn3-Sn3 103.67(8), C31-Sn3-Sn3 105.72(8), Sn1-C1-C2 119.5(2), Sn1-C1-C6 123.5(2), Sn1-C7-C8 118.3(2), Sn1-C7-C12 124.9(2), Sn2-C13-C14 122.7(2), Sn2-C13-C18 119.8(2), Sn2-C19-C20 122.1(2), Sn2-C19-C24 120.5(2), Sn3-C25-C26 120.2(2), Sn3-C25-C30 122.2(2).

The terminal Sn1-Sn2 bond length with 2.8818(3) Å is about 0.05 Å longer than between Sn2-Sn3 (2.8363(2) Å, which is a consequence of the negative charge located at terminal tin atom Sn1. On the other hand the anionic charge at Sn1 has no notable effect on the Sn1-C bond distances, where no significant difference with respect to Sn-C bonds around neutral tin atoms can be detected.

In the course of reaction **(1.4)** the methylated species $Ph_2SnMe_2$ and the monoanionic distannane $LiPh_2SnSnPh_2H$ are formed. This dimeric compound is an important building block in further reactions towards the dianionic chains with exclusively even number of tin atoms which are discussed later.

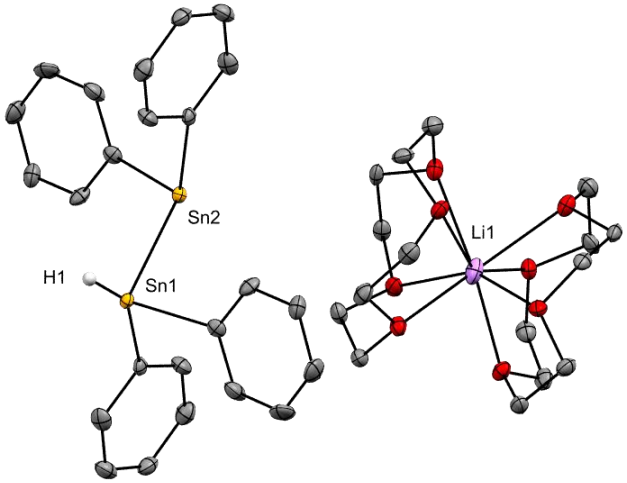


**Figure 4.2** Molecular structure of **$[Ph_2SnSnPh_2H]^-[Li(12\text{-crown-}4)_2]^+$** Hydrogens are omitted for clarity. Ellipsoids shown at a probability of 30%. Selected bond lengths [Å] and angles [°]: Sn1-C7 2.233(5), Sn1-C1 2.255(7), Sn1-Sn2 2.837(1), Sn1-H1 1.479(6), Sn2-C7 2.158(6), Sn2-C1 2.169(7); H1-Sn1-Sn2 96.08., Sn2-Sn1-H1 126.8.

The Sn1-Sn2 bond distance in $HPh_2SnSnPh_2^-$ with 2.837(1) Å, where Sn2 is anionic, is equal to the bond length between neutral tin atoms described in the previously discussed dianion $[Ph_{12}Sn_6]^{2-}$. The Sn1-C bonds (2.255 Å) are with 0.1 Å somewhat longer than the Sn-C bonds (2.158 Å).

2.) Deprotonation agent: **Methyllithium;** Solvent: **Diglyme**

The order for the reactions is for both routes the same. At first $Ph_2SnH_2$ was fully dissolved in diglyme (Bis(2-methoxyethyl)ether), followed by dropwise addition of MeLi to the reaction mixture. After a day at room temperature the mother liquor turned from yellow to a dark green and colorless precipitate (lithium salt) formed. However, no identifiable product was isolated from reactions **1.5** and **1.6**.

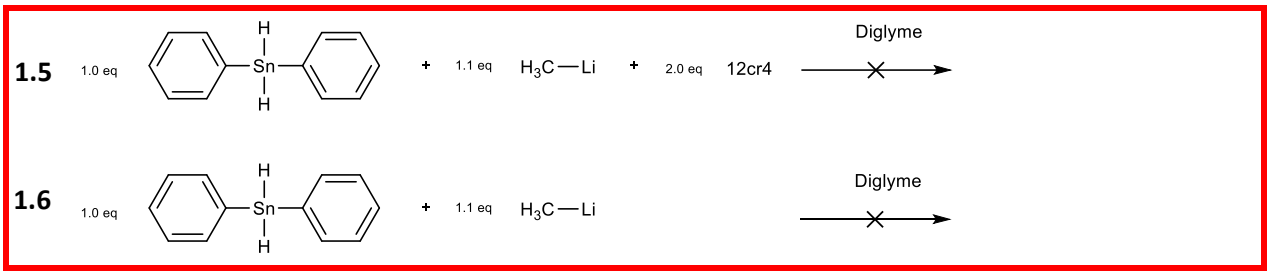


**Scheme 4.4** Reactions **(1.5)(1.6)** of $Ph_2SnH_2$ with MeLi in diglyme

3.) Deprotonation agent: **MeLi**; Solvent: **DME**

In this reaction types in general diphenyltin dihydride was fully dissolved in DME followed by dropwise addition of 12cr4. Finally, a respective amount of MeLi was added at room temperature.

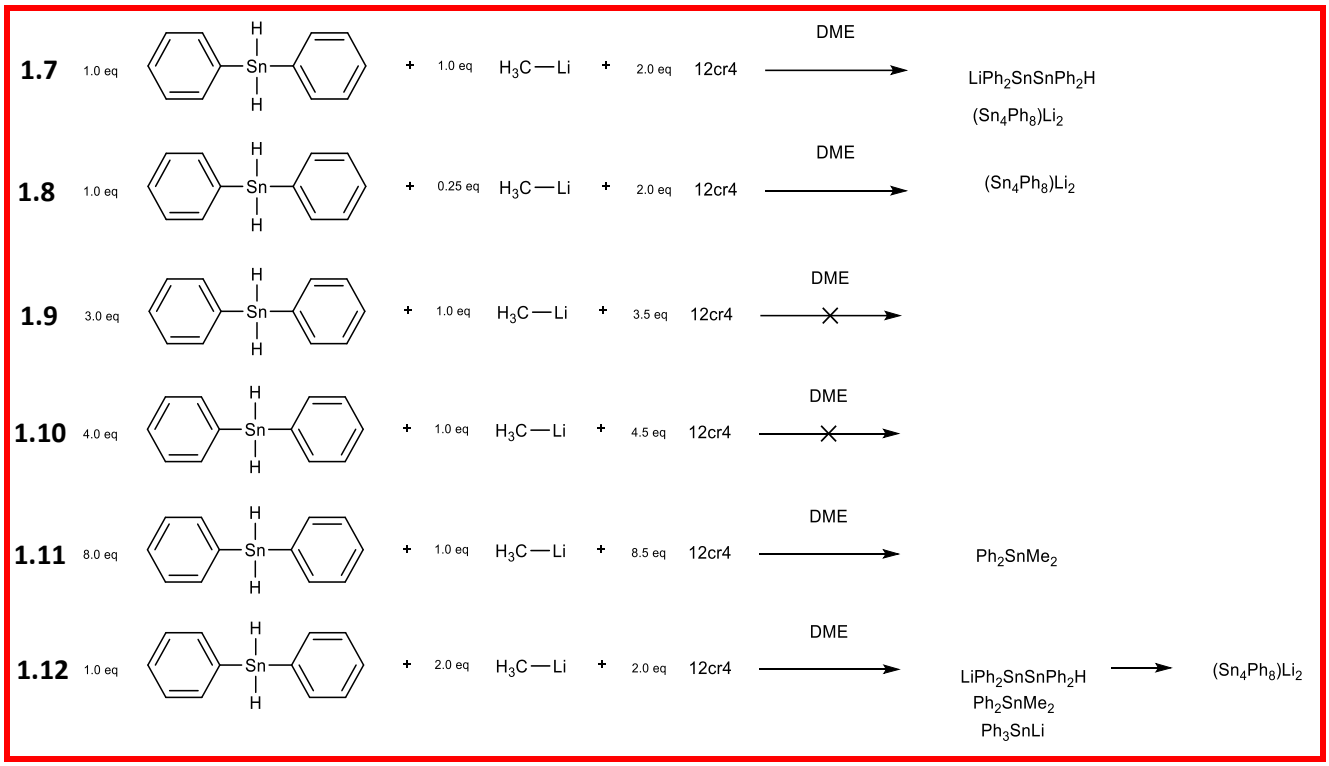


**Scheme 4.5** Reactions **(1.7)-(1.12)** of $Ph_2SnH_2$ with MeLi in DME

Reaction **(1.7)** ($Ph_2SnH_2$:MeLi = 1:1) initially gave a light-yellow solution. After 2 days, the mother liquor had turned deep red and violet crystals formed which were confirmed as $(Sn_4Ph_8)Li_2$ via X-ray structure analysis. A $^{119}Sn$ NMR spectrum of the supernatant solution showed the formation of distannane monoanion $HPh_2SnSnPh_2^-$.

In reaction **(1.8)** different ratios of the educt were chosen and the reaction mixture was kept at -30°C after complete addition. The next day violet crystals in a deep red solution had formed. X-ray structure analysis again showed the formation of $(Sn_4Ph_8)Li_2$.

In reactions **(1.9)** and **(1.10),** excess of diphenyltin dihydride with high molar ratios of 12cr4 lead to no isolable compounds. In both cases a colorless precipitate, most likely of LiH had formed from a light-yellow solution.

Surprisingly, in reaction **(1.11)**, where even higher amounts of $Ph_2SnH_2$ were investigated, the reaction solution immediately turned dark yellow. After 24 hours, a clear orange solution was obtained, for which again $^{119}$Sn-NMR spectroscopy showed the formation of $Ph_2SnMe_2$.

The last experiment **(1.12)** in this series was made with equal equivalents of MeLi and 12cr4, a light-yellow solution formed. After 24 hours, a $^{119}$Sn-NMR spectrum was made, where signals of $LiPh_2SnSnPh_2H$, $Ph_2SnMe_2$ and $Ph_3SnLi$ were detected. From that after 2 weeks again violet crystals of $(Sn_4Ph_8)Li_2$ had formed. Storage of these reaction mixtures for extended periods of time at -30°C yielded small amount of $Ph_3SnLi$.

Interestingly, in any case no dianionic product other than $(Sn_4Ph_8)Li_2$ was obtained from reactions between $Ph_2SnH_2$ and MeLi in DME as solvent and in the presence of 12cr4. However, evidence for the occurrence of redistribution reactions (i.e. isolation of $Ph_3SnLi$) and substitution rather deprotonation reactions (formation of $Ph_2SnMe_2$) in solution was found.

In this reaction series it could be seen that the ratio of the starting material has no effect on the formation of $(Sn_4Ph_8)Li_2$ .

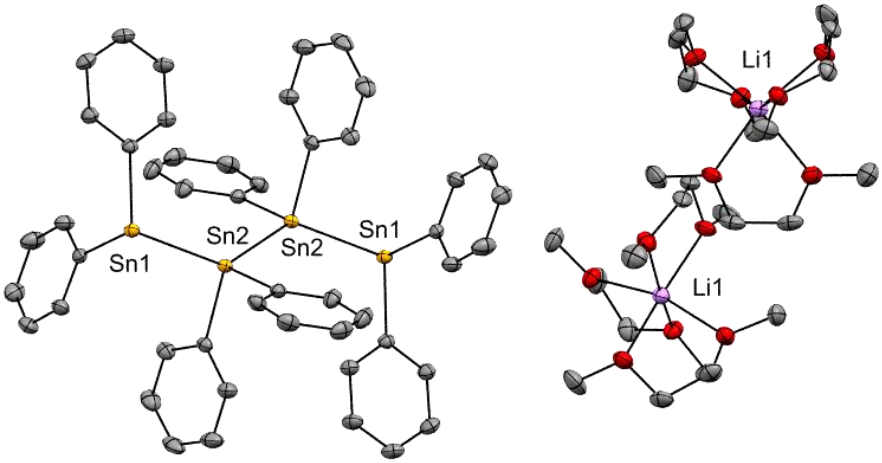


**Figure 4.3** Molecular structure of $[Ph_8Sn_4]^{2-}[Li(DME)_2]_2^+$ Hydrogens are omitted for clarity. Ellipsoids shown at a probability of 30%. Selected bond lengths [Å] and angles [°]: Sn1-Sn2 2.8774(1), Sn1-C1 2.217(1), Sn1-C7 2.216(1), Sn2-C19 2.184(1), Sn2-C13 2.192(1), Sn2-Sn2 2.8431(1), Sn1-Sn2 .8774(1), Sn1-C1 2.217(1), Sn1-C7 2.216(1), Sn2-C19 2.184(1), Sn2-C13 2.192(1); Sn2-Sn1-C7 101.78(3), C1-Sn1-C7 94.79(5), Sn1-Sn2-C19 104.96(4), Sn1-Sn2-C13 104.51(4), Sn1-Sn2-Sn2 134.00, C19-Sn2-C13 97.03(5), C19-Sn2-Sn2 104.95(4), C13-Sn2-Sn2 105.57(4), Sn2-C19-C24 124.2(1), Sn2-C19-C20 118.5(1), Sn1-C1-C2 123.6(1), Sn1-C1-C6 120.0(1), Sn2-C13-C18 122.7(1), Sn2-C13-C14 120.1(1), Sn1-C7-C12 117.0(1), Sn1-C7-C8 126.3(1), Sn2-Sn1-C1 92.78(4), Sn2-Sn1-C7 101.78(3), C1-Sn1-C7 94.79(5), Sn2-Sn2-Sn1 134.00, Sn2-Sn2-C19 104.95(4), Sn2-Sn2-C13 105.57(4), Sn1-Sn2-C19 104.96(4), Sn1-Sn2-C13 104.51(4), C19-Sn2-C13 97.03(5), Sn2-C19-C24 124.2(1), Sn2-C19-C20 118.5(1), Sn1-C1-C2 123.6(1), Sn1-C1-C6 120.0(1), Sn2-C13-C18 122.7(1), Sn2-C13-C14 120.1(1).

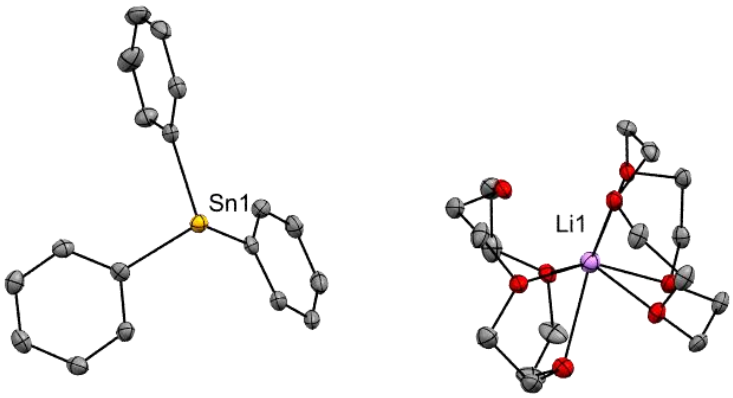


**Figure 4.4** Molecular structure of **$[Ph_3Sn]^-[Li(12cr4)_2]^+$** Hydrogens are omitted for clarity. Ellipsoids shown at a probability of 30%. Selected bond lengths [Å] and angles [°]: Sn1-C1 2.231(2), Sn1-C7 2.225(2), Sn1-C13 2.246(3); C1-Sn1-C7 97.75(9), C1-Sn1-C13 92.80(8), C7-Sn1-C13 98.58(8), Sn1-C1-C2 119.1(2), Sn1-C1 C6 124.6(2), Sn1-C7-C8 125.3(2), Sn1-C7-C12 118.9(2), Sn1-C13-C14 126.8(2), Sn1-C13-C18 117.3(2).

However, when $Ph_2SnH_2$, MeLi and 12cr4 were used in a ratio of 1:1, 1:2 under otherwise identical reaction conditions, a neutral polystannane **-[$Ph_2Sn$]-** was isolated as a crystalline material suitable for single crystal X-ray structure analysis.

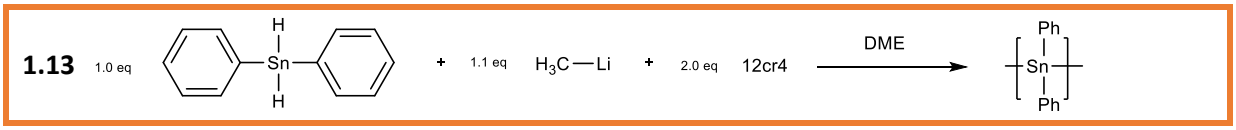


**Scheme 4.6** Reaction **(1.13)** of $Ph_2SnH_2$ with MeLi in DME

In that pathway, $Ph_2SnH_2$ was fully dissolved in 10 mL DME, 12cr4 was added and finally MeLi was added to the reaction mixture, to initially yield a bright yellow, slightly turbid solution. Two hours later, the mother liquor turned orange and small, dichroic yellow/blueish crystals start to form. After 24 hours, the crystals had significantly grown, where upon the mother liquor was put in a new vial and kept in the fridge under -30°C. The next day also, from the supernatant another batch of small yellow/blueish crystals formed. The X-ray structure analysis showed that in both samples polystannane poly[$Ph_2Sn$] had cocrystallized as linear chains with 12cr4 molecules filling the voids of the crystal lattice.

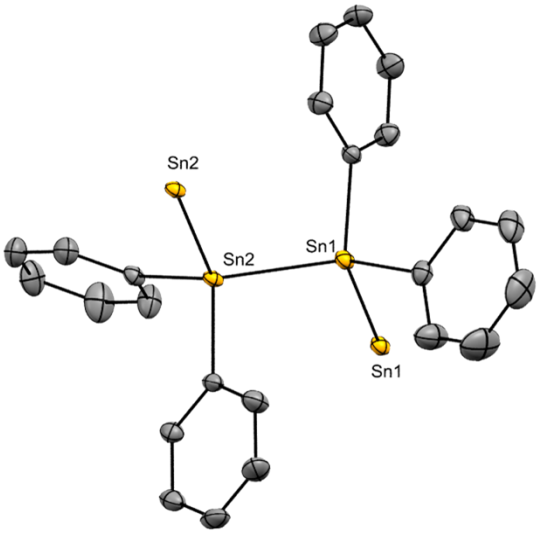


**Figure 4.5** Molecular structure of -**[$Ph_2Sn$]-** Hydrogens are omitted for clarity Ellipsoids shown at a probability of 30%. Selected bond lengths [Å] and angles [°]: Sn1-C1 2.156(3), Sn1-Sn2 2.8209(6), Sn1-C4 2.154(4), Sn1-Sn1 2.8203(7), Sn2-C13 2.165(4), Sn2-C19 2.147(3), Sn2-Sn2 2.8131(7); C1-Sn1-Sn2 106.3(1), C1-Sn1-C4 106.0(1), C1-Sn1-Sn1 108.2(1), Sn2-Sn1-C4 107.7(1), Sn2-Sn1-Sn1 118.14(1), C4-Sn1-Sn1 109.7(1), Sn1-C1-C2 120.7(3), Sn1-C1-C5 120.8(3), Sn1-Sn2-C13 106.1(1), Sn1-Sn2-C19 108.1(1), Sn1-Sn2-Sn2 118.17(1), C13-Sn2-C19 105.8(1), C13-Sn2-Sn2 108.7(1), C19-Sn2-Sn2 109.3(1), Sn1-C4-C8 121.8(3), Sn1-C4-C12 120.2(3), Sn2-C13-C14 121.3(3), Sn2-C13-C18 120.3(3), Sn2-C19-C20 119.2(3), Sn2-C19-C24 123.1(3).

The Sn-Sn bond lengths are all in the same range and rather short between 2.8209 to 2.8131 Å. Also, the Sn-C bonding does not differ notably.

From mother liquor, a small amount of a second compound was isolated, [$Ph_7Sn_3$]Li. Its chemical constitution was determined by crystal structure analysis. This compound may result from rearrangement reactions via phenyl group migration.

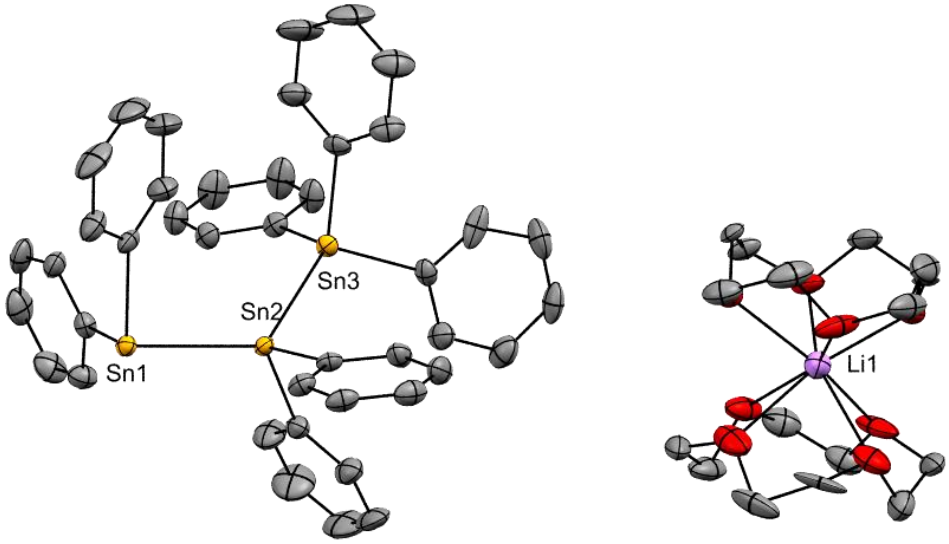


**Figure 4.6** Molecular structure of **[$Ph_7Sn_3$]**-Hydrogens are omitted for clarity. Ellipsoids shown at a probability of 30%. Selected bond lengths [Å] and angles [°]: C1-Sn1 2.221(9), Sn1-Sn2 2.8662(7), Sn1-C7 2.206(6), Sn3-Sn2 2.8131(6), Sn3-C31 2.173(6), Sn3-C25 2.169(9), Sn3-C38 2.169(9), Sn2-C13 2.177(7), Sn2-C19 2.174(9); Sn1-C1-C2 122.6(6), Sn1-C1-C6 120.0(6), C1-Sn1-Sn2 96.1(2), C1-Sn1-C7 97.0(3), Sn2-Sn1-C7 94.0(2), Sn2-Sn3-C31 120.4(2), Sn2-Sn3-C25 114.3(2), Sn2-Sn3-C38 112.7(2), C31-Sn3-C25 105.2(3), C31-Sn3-C38 100.3(3),

C25-Sn3-C38 101.5(3), Sn1-Sn2-Sn3 125.23(2), Sn1-Sn2-C13 117.3(2), Sn1-Sn2-C19 111.2(2), Sn3-Sn2-C13 94.5(2), Sn3-Sn2-C19 105.0(2), C13-Sn2-C19 99.8(3), Sn1-C7-C8 126.6(7), Sn1-C7-C12 117.7(6), Sn2-C19-C20 123.1(6), Sn2-C19-C24 118.9(6)

In the remaining mother liquor, the formation of the substitution product $Me_2Ph_2Sn$ was confirmed by $^{119}Sn$ NMR spectroscopy. The consumption of the MeLi in a substitution reaction accounts for the lack of other anionic oligotin fragments.

4.) Deprotonation agent: **MeLi**; Solvent: **$Et_2O$**

In a series of reactions, the influence of the weakly coordinating solvent diethyl ether was investigated with the task to isolate the initially formed deprotonated species $Ph_2HSnLi$. In all cases, methyl lithium was dissolved in diethyl ether followed by addition of a sequestering agent e.g. 12cr4. Afterwards a solution of diphenyltin dihydride in the same solvent was slowly added.

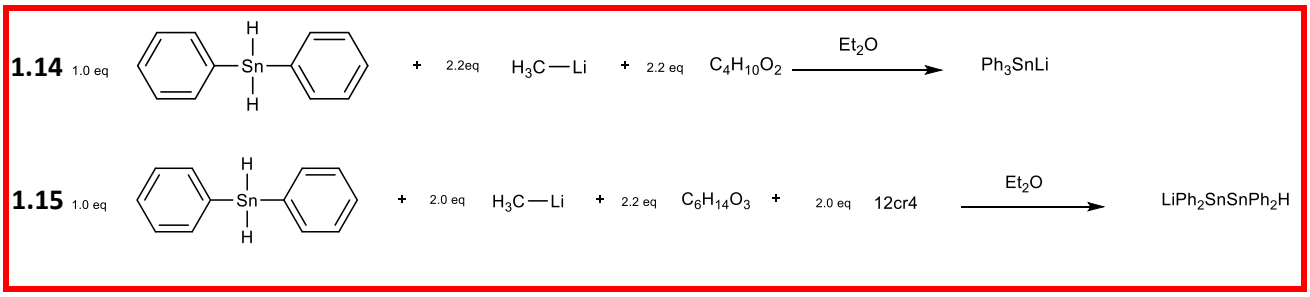


**Scheme 4.7** Reactions **(1.14)(1.15)** of $Ph_2SnH_2$ with MeLi in $Et_2O$

In the first attempt, to isolate $Ph_2HSnLi$ shown above, a clear, light brown reaction mixture was obtained. $^{119}Sn$-NMR spectroscopy showed the predominant formation of $Ph_3SnLi$ among other reaction products.

Reaction **(1.15)** was carried out, where additionally 12cr4 was added. After 24h a colorless precipitate formed, which was recrystallized in DME at -30°C. After 2 weeks small orange crystals were isolated. A $^{119}Sn$-NMR spectroscopy showed the formation of $HPh_2SnSnPh_2Li$.

Finally, the very slow addition of a precooled solution of diphenyltin dihydride to a previously prepared and also precooled (-30°C) solution of MeLi and 2.0 equivalents of 12cr4 in $Et_2O$ yielded the desired anion $Ph_2SnH^-$ as colorless crystals.

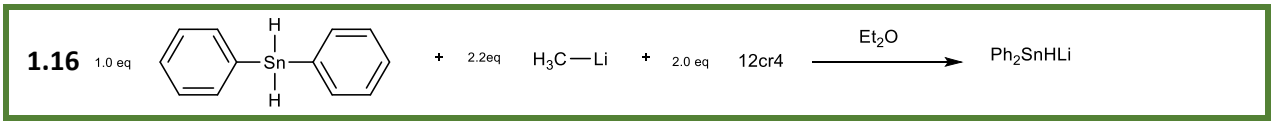


**Scheme 4.8** Reaction **(1.16)** of $Ph_2SnH_2$ with MeLi in $Et_2O$

A second crop of crystals were isolated from the supernatant upon cooling to -30°C. A X-ray crystal structure analysis confirmed the formation of **$Ph_2SnH^-$**. The isolation of the elusive anion $Ph_2SnH^-$ as its lithium salt, is a crucial step in understanding the formation of oligostannadiides $[Ph_2Sn)_n]^{2-}$. The previously described formation of $LiPh_2SnSnPh_2H$ is readily explicable via dimerization of $Ph_2SnHLi$ under LiH elimination. The much more stable anion $LiPh_2SnSnPh_2H$ continues to oligomerize into a series of even-numbered dianions $[Ph_8Sn_4]^{2-}$, $[Ph_{12}Sn_6]^{2-}$ and $[Ph_{16}Sn_8]^{2-}$. Alternatively, $Ph_2SnH^-$ was reacted with additionally added equivalents of diphenyltin dihydride. The reaction proceeds under evolution of dihydrogen and ultimately yielded the $[Ph_8Sn_4]^{2-}$ and $[Ph_{12}Sn_6]^{2-}$.

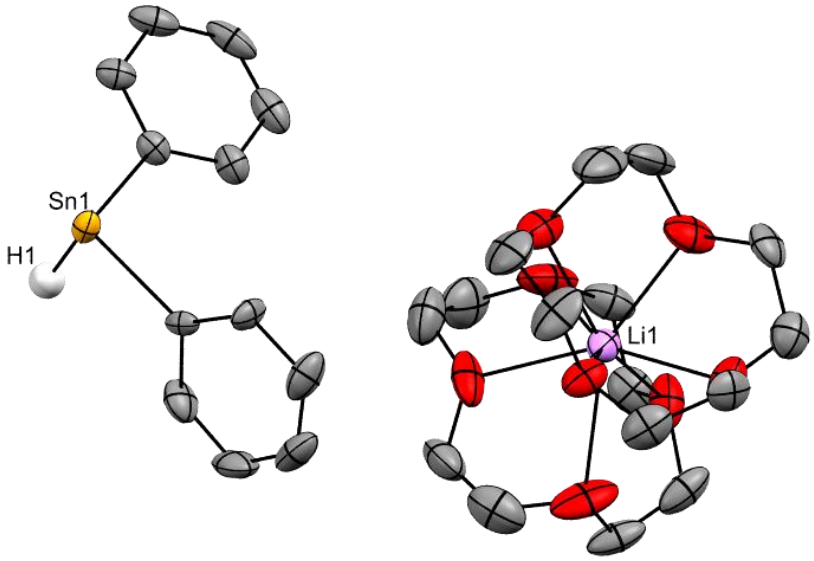


**Figure 4.7** Molecular structure of **$[Ph_2SnH]^-$ $[Li(12cr4)_2]^+$** Hydrogens are omitted for clarity. Ellipsoids shown at a probability of 30%. Selected bond lengths [Å] and angles [°]: Sn1-Cn1 2.225(3), Sn1-H1 1.66(3), Sn1-C7 2.220(1); C2-C1-Sn1 125.4(2), C6-C1-Sn1 118.2(2), C1-Sn1-H1 89(1), C1-Sn1-C7 97.8(4), H1-Sn1-C7 89(1), Sn1-C7-C8 123(1), Sn1-C7-C12 126(1).

In the following figure an overview of the reactions $Ph_2SnH_2$ with MeLi in THF, DME and $Et_2O$ provided.

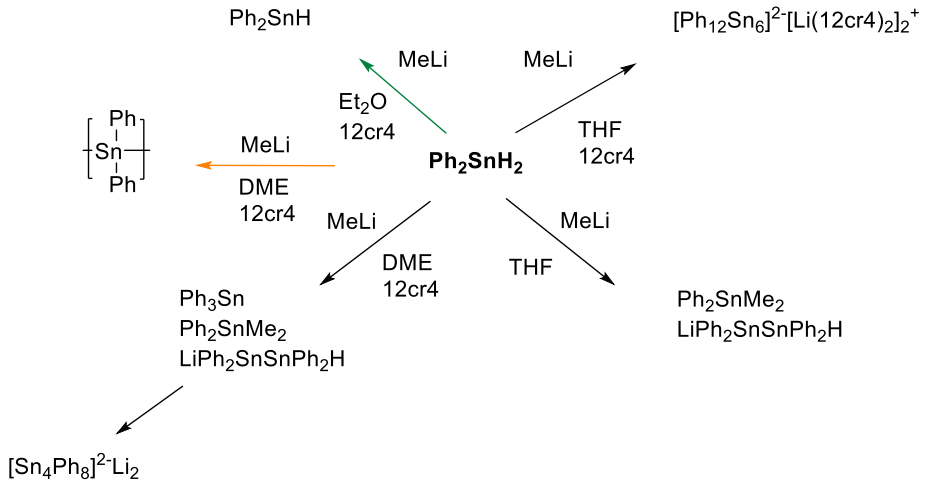


**Figure 4.8** Overview of the reactions of $Ph_2SnH_2$ with MeLi in different solvents

5.) Deprotonation agent: ***n*-BuLi**; Solvent: **Diglyme**

In order to assess the influence of basicity/nucleophilicity on the metalation of diphenyltin dihydride, butyl lithium was investigated as an alternative metalating reagent. The first distinction to the reactions using MeLi become noticeable by adding diphenyltin dihydrate to *n*-BuLi in Diglyme. In contrast to the reactions with methyl lithium, the reaction showed no apparent gas evolution but only a color change to a clear deep yellow tone. After 2 days, the color of the reaction mixture had changed to a deep red from which cubic, violet crystals had precipitated. In accordance with a slower deprotonation of $Ph_2SnH_2$ by *n*-BuLi, dehydrogenative coupling of $Ph_2SnH_2$ leads to the formation of $Ph_{12}Sn_6Li_2$ as the starting material is not entirely consumed by *n*-BuLi but remains in solution to react with $Ph_2SnHLi$.

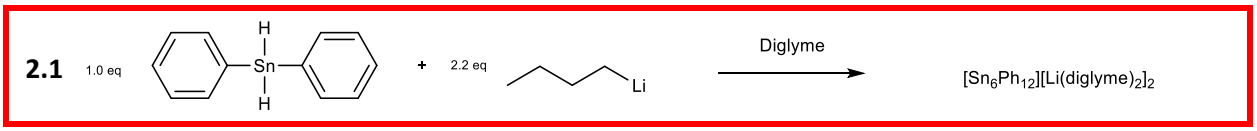


**Scheme 4.9** Reaction **(2.1)** of $Ph_2SnH_2$ with *n*-BuLi in diglyme

6.) Deprotonation agent: ***n*-BuLi**; Solvent: **DME**

In the following synthesis, two additional chelating agents, DME and 12cr4, were used to break up the *n*-BuLi hexamers and increase reactivity. After complete addition of $Ph_2SnH_2$ the reaction mixture turned light-yellow. $^{119}$Sn-NMR spectroscopy showed that in the solution the Sn-Sn dimer ($LiPh_2SnSnPh_2H$) and the buthylated ($Ph_2SnBu_2$) species form. Five days later,

the mother liquor had turned orange and small black-violet crystals formed on the bottom of the vial. X-ray analysis showed, that the octameric dianion $[Sn_8Ph_{16}][Li(12cr4)_3]_2$ had formed. However, this gets conform with the results of point 5. The isolation of the extended structure is probably a consequence of the increased solubility of the anionic intermediates in the presence of complexing agents.

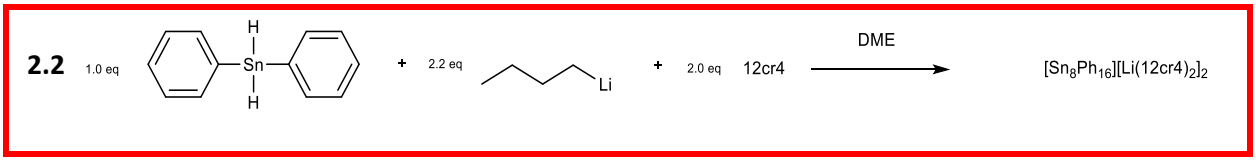


**Scheme 4.10** Reactions **(2.2)** of $Ph_2SnH_2$ with *n*-BuLi in DME

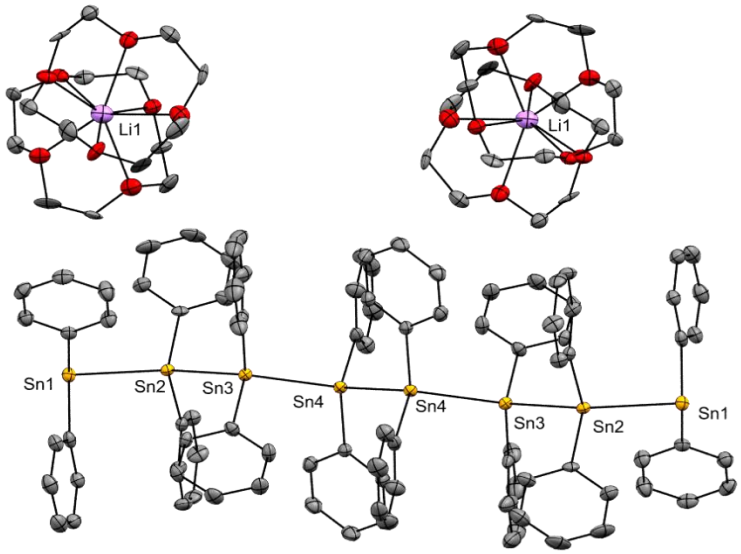


**Figure 4.9** Molecular structure of **$[Sn_8Ph_{16}][Li(12cr4)_2]_2$** Hydrogens are omitted for clarity. Ellipsoids shown at a probability of 30%. Selected bond lengths [Å] and angles [°]: Sn1-C1 2.206(5), Sn1-Sn2 2.8900(4), Sn1-C7 2.220(6), Sn2-Sn3 2.8238(4), Sn2-C13 2.184(6), Sn2-C19 2.169(5), Sn3-Sn4 2.8128(4), Sn3-C25 2.169(5), Sn3-C31 2.155(6), Sn4-C37 2.165(6), Sn4-C43 2.158(5), Sn4-Sn4 2.8225(4); Sn1-Sn2-Sn3 127.41(1), Sn2-Sn3-Sn4 127.18(2).

The bond distance between the anionic Sn1 to Sn2, with a length of 2.8900(4) Å, is about 0.07 Å longer than the Sn2-Sn3 bond (2.8238(4) Å). One more, the negative charge of the tin atom has less effect on the bond length between the Sn-C bond. The results are around 2.2 Å for every Sn-C distance in $[Sn_8Ph_{16}]^{2-}$.

7.) Deprotonation agent: ***n*-BuLi**; Solvent: **$Et_2O$**

In agreement with the lower donor strength of diethyl ether in comparison to the use of DME or diglyme as solvent, the reaction of $Ph_2SnH_2$ with *n*-BuLi in $Et_2O$ in the presence of two equivalents of 12cr4 resulted in the formation of tetrameric $Ph_8Sn_4Li_2$. The reaction in diethyl ether turned, after the addition of $Ph_2SnH_2$ to the reagents, dark yellow and an oily precipitate formed. The next day the ether phase turned completely colorless and small orange crystals

of $[Sn_4Ph_8][Li(12cr4)_2]_2$ had formed. Similar to the observations when MeLi was used as base, $^{119}Sn$ NMR spectroscopy of the supernatant indicated the formation of $HPh_2SnSnPh_2Li$ and $Bu_2SnPh$.

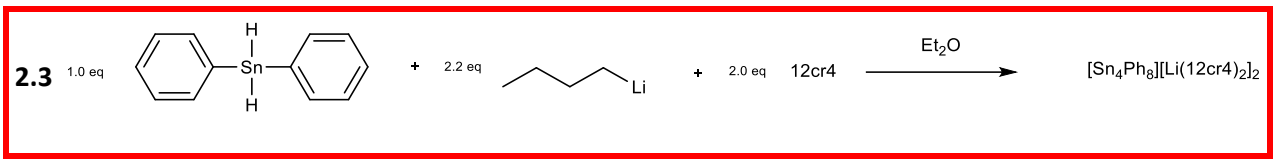


**Scheme 4.11** Reactions **(2.3)** of $Ph_2SnH_2$ with *n*-BuLi in diglyme

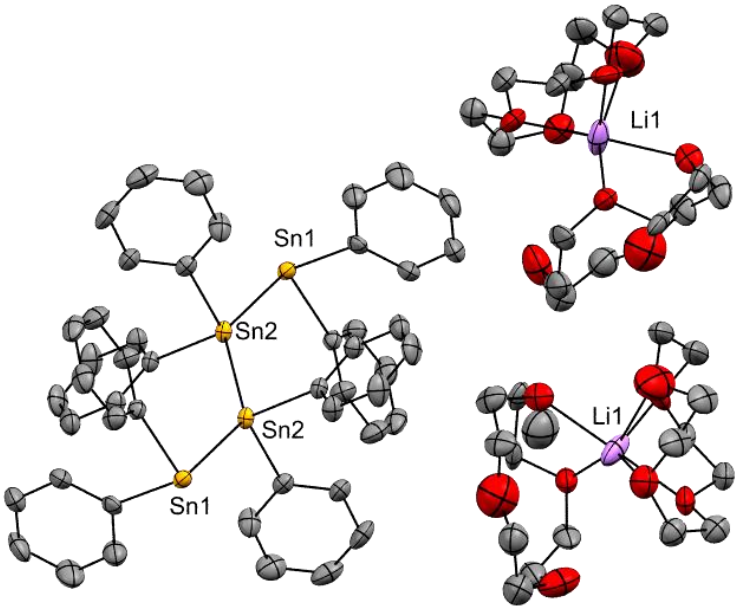


**Figure 4.10** Molecular structure of **$[Sn_4Ph_8][Li(12cr4)_2]_2$** Hydrogens are omitted for clarity. Ellipsoids shown at a probability of 30%. Selected bond lengths [Å] and angles [°]Sn1-C1 2.220(1), Sn1-Sn2 2.8603(6), Sn1-C7 2.223(1), Sn2-C13 2.183(1), Sn2-C19 2.187(1), Sn2-Sn2 2.8210(4), Sn1-C1 2.220(1), Sn1-Sn2 2.8603(6), Sn1-C7 2.223(1), Sn2-C13 2.183(1), Sn2-C19 2.187(1); Sn1-Sn2-Sn2 135.43(2), Sn2-Sn2-Sn1 135.43(2).

The dianion $[Sn_4Ph_8]^{2-}$ once again displays an elongated terminal Sn-Sn bond at 2.8603(6) Å (c.f. 2.8774(1) Å in the respective DME complex $[Sn_4Ph_8][LiDME_3]_2$) and a slightly shorter central bond of 2.8210(4) Å (2.8431(1) in $[Sn_4Ph_8][LiDME_3]_2$).

8.) Deprotonation agent: **LiHMDS**; Solvent: **THF**

As an alternative to alkyllithium reagents, the non-nucleophilic base lithium hexamethyldisilazanide, LiHMDS, was investigated. As the reagent is sterically more hindered than MeLi or *n*-BuLi, a lower reactivity in deprotonation reactions was expected. $Ph_2SnH_2$ was

dissolved in 10 mL THF to yield a light-yellow solution to which 1.0 equivalents of LiHMDS were added. After three days, small orange crystals formed from an orange mother liquor. X-ray structure analysis showed the formation of $^{cy}[Sn_6Ph_{10}][Li(THF)_2]_2$.

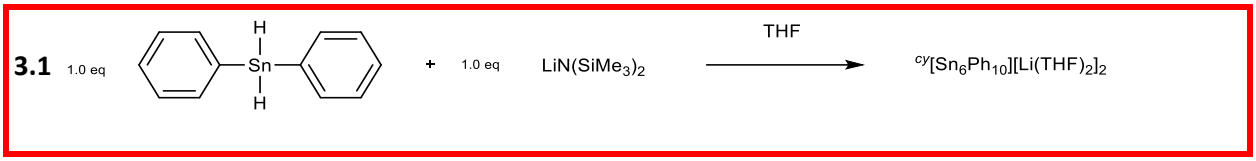


**Scheme 4.12** Reactions **(3.1)** of $Ph_2SnH_2$ with LiHMDS in THF

Similar to observations with *n*-BuLi, tin-tin formation is the predominant reaction pathway. However, LiHMDS also induces redistribution reactions of phenyl substituents. Hence, a cyclic hexamer rather than linear dianions are obtained. In previous experiments, the anion $Ph_5Sn_2Li$ was obtained upon concentration of the reaction mixture and cooling to -30°C.

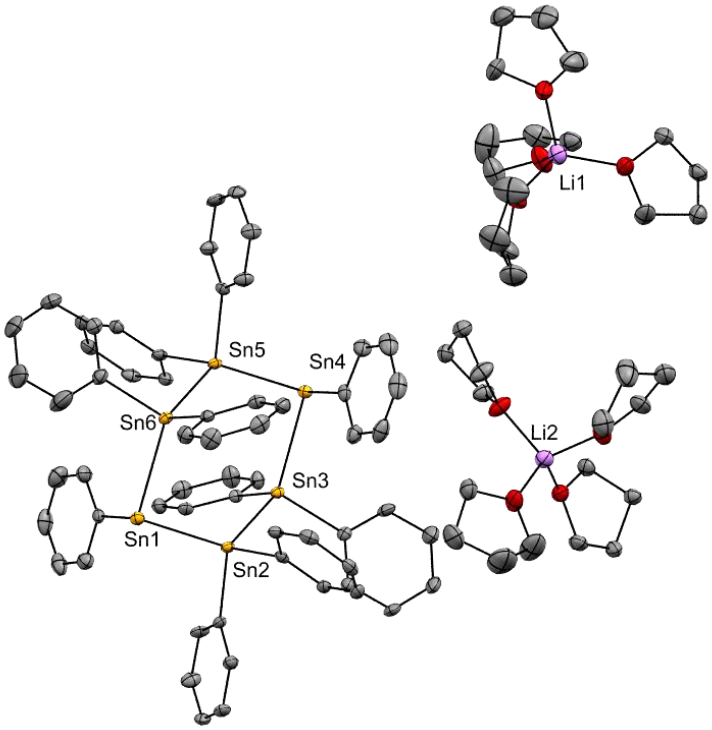


**Figure 4.11** Molecular structure of $^{cy}$**[Ph$_{10}$Sn$_6$]$^{2-}$ [Li·4THF]$_2^+$.** Hydrogens are omitted for clarity. Ellipsoids shown at a probability of 30%. Selected bond lengths [Å] and angles [°]: Sn1-C1 2.221(4), Sn1-Sn2 2.8489(7), Sn1-Sn6 2.8432(6), Sn2-Sn3 2.8129(8), Sn2-C7 2.192(4), Sn2-C13 2.182(4), Sn3-Sn4 2.8459(6), Sn3-C19 2.191(4), Sn3-C25 2.175(4), Sn4-Sn5 2.8450(7), Sn4-C31 2.221(4), Sn5-Sn6 2.8104(8), Sn5-C37 2.188(4), Sn5-C43 2.182(4), Sn6-C49 2.193(4), Sn6-C55 2.182(4); Sn1-Sn2-Sn3 124.45(2), Sn3-Sn4-Sn5 92.86(2), Sn4-Sn5-Sn6 124.68(2), Sn1-Sn6-Sn5 127.12(2).

The crystal structure of $^{cy}[Ph_{10}Sn_6]^{2-}$ anion shows no interaction to the $[Li{\cdot}4THF]_2^+$ cation. The Sn-Sn bonds attached to the anionic Sn1 atom are 2.8489(7) and 2.8432(6) Å, to the anionic Sn2 atom 2.8459(6) and 2.8450(7) Å. These bond lengths are around 0.03 Å longer than the distance between tetra-coordinated Sn atoms like Sn2-Sn3 (2.8129(8) Å.

**Table 4.1.1** Overview of average bond length [Å] and angles [°] of the anionic tin compounds

| | **$Sn^-$-Sn** | **Sn-Sn** | **$Sn^-$-C** | **Sn-C** | **Sn-H** | **Sn-Sn-Sn** |
|---|---|---|---|---|---|---|
| | [Å] (averg.) | [Å] (averg.) | [Å] (averg.) | [Å] (averg.) | [Å] (averg.) | [°] (averg.) |
| **$Ph_2SnH^-$** | - | - | 2.225(3) | 2.220(1) | 1.66(3) | - |
| **$[Ph_3Sn]^-$** | - | - | 2.225(2) | 2.2346(3) | - | - |
| **$[Ph_2SnSnPh_2H]^-$** | 2.837(1) | - | 2.255(7) | 2.158(6) | 1.479(6) | - |
| **$[Ph_7Sn_3]^-$** | 2.8662(7) | 2.8131(6) | 2.214(8) | 2.172(8) | - | 125.23(2) |
| **$[Ph_8Sn_4]^{2-}$** | 2.8774(1) | 2.8431(1) | 2.217(1) | 2.188(1) | - | 134.00 |
| **poly -$Ph_2Sn$-** | - | 2.8203(7) | 2.155(4) | 2.156(4) | - | 118.14(1) |
| **$[Ph_{12}Sn_6]^{2-}$** | 2.8777(9) | 2.8224(9) | 2.218(9) | 2.180(2) | - | 128.72(3) |
| **$[Ph_{16}Sn_8]^{2-}$** | 2.8900(4) | 2.8183(4) | 2.213(6) | 2.167((6) | - | 127.41(1) |
| **$^{cy}[Sn_6Ph_{10}]^{2-}$** | 2.8458(7) | 2.8117(7) | 2.221(4) | 2.192(4) | - | 117.28(2) |

In Table 4.1.1 all compounds investigated by X-ray crystallography are summarized and compared. In the first row of the table the bond length of anionic Sn with neutral Sn are given. It is clearly visible that the tin-tin distances are elongated when bonding to a negatively charged tin atom is involved as compared to Sn-Sn bonds between neutral tin atoms. The bond elongation is by far less pronounced for tin carbon distances. Similarly, the angles around negatively charged tin atoms are smaller as compared to the coordination environment around neutral tin atoms, where angles are typically close to the ideal tetrahedral angle. The Sn-H bond length in the anions $Ph_2SnH^-$ and $Ph_2SnSnPh_2H^-$ between Sn-H is similar in both cases.

The Sn-Sn-Sn angle decreases the longer the Sn anionic chain is. In $[Ph_8Sn_4]^{2-}$ the largest angle at 134.00° is detected, which decrease over $[Ph_{12}Sn_6]^{2-}$ with 128.72(3)° to $[Ph_{16}Sn_8]^{2-}$ with 127.41(1)°. The smallest angles are observed for the neutral polymer poly-$[Ph_2Sn]$- at 118.14(1)° and in the cyclic species $^{cy}[Sn_6Ph_{10}]^{2-}$ at 117.28(2)°.

**Table 4.1.2** Overview of the observed $^{119}$Sn-NMR-data of the anionic tin compounds

| **$^{119}$Sn-NMR shift ppm** | **Assignment** |
|---|---|
| (-0.2)-(-0.7) | $Ph_2SnMe_2$ |
| -(60) | $Ph_2SnMe_2$ |
| (-106)-(-109) | $Ph_3SnLi$ |
| -128,2 | $Ph_4Sn$ |
| -178 | $Ph_2SnHLi$ |
| -180 | $Ph_2HSnSnPh_2Li/Me_3SnLi$ |
| -182 | $Ph_2HSnSnPh_2Li/Me_3SnLi$ |
| -188 | $Ph_2HSnSnPh_2Li$ |
| -194 | $Ph_2HSnSnPh_2Li$ |
| -208 | $^{cy}[Ph_{10}Sn_6]^{2-}$ |

In Table 4.1.2 the observed $^{119}$Sn-NMR data from the anionic tin species are summarized. The classification was compared with literature. [28,29,30,31]

### 4.1.2 Metallation of $Ph_2SnH_2$ by alkali metals

In order to extend the metallation chemistry of diphenyltin dihydride to group 1 metals other than lithium $Ph_2SnH_2$ was directly reacted with alkali metals in various solvents including THF, DME, diglyme and benzene. Furthermore, the addition of sequestering agents and strong donor molecules like 12cr4, 15cr5, 18cr6, dibenzo18cr6 or acetonitrile was studied. In this investigations, small pieces of alkali metals (Li, Na, K, Rb, Cs) were added to solutions of diphenyltin dihydride. Hydrogen evolution started immediately at the surface of the alkali metals, followed by rapid colour change which initiated on the surface of the metal pieces. In the course of the reaction, the metal was consumed to give deeply colored reaction mixtures from which crystalline material typically precipitated within a few days. The reaction of $Ph_2SnH_2$ with Li in benzene in the presence of 12cr4 yields violet crystals in a yellow mother liquor. X-ray crystallography show that $[Ph_{16}Sn_8]^{2-}$ $[Li\ (12cr4)_2]_2^+$ formed (see Scheme 4.13). The structure is equal to the X-ray structure seen in Figure 4.9.

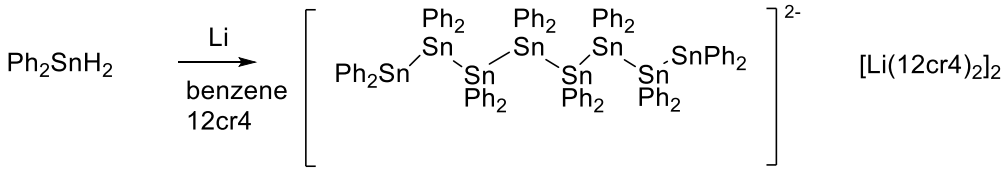


**Scheme 4.13** Formation of **$[Ph_{16}Sn_8]^{2-}$ $[Li\ (12cr4)_2]_2^+$**

When the reaction is carried out in neat DME instead of benzene, hexameric $[Ph_{12}Sn_6]^{2-}$ $[Li\ (DME)_3]_2^+$ forms.

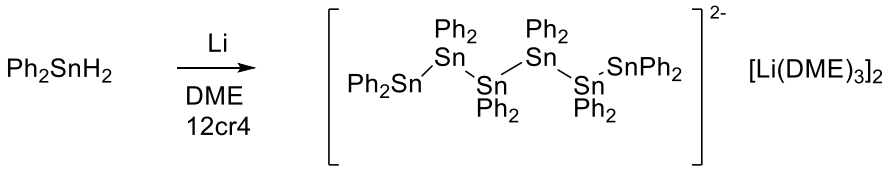


**Scheme 4.14** Formation of **$[Ph_{12}Sn_6]^{2-}$ $[Li\ (DME)_3]_2^+$**

The bond between anionic Sn1 and Sn2 is with 2.8763(9) Å, 0.05 Å larger than between neutral atoms Sn2-Sn3 (2.8207(9) Å).

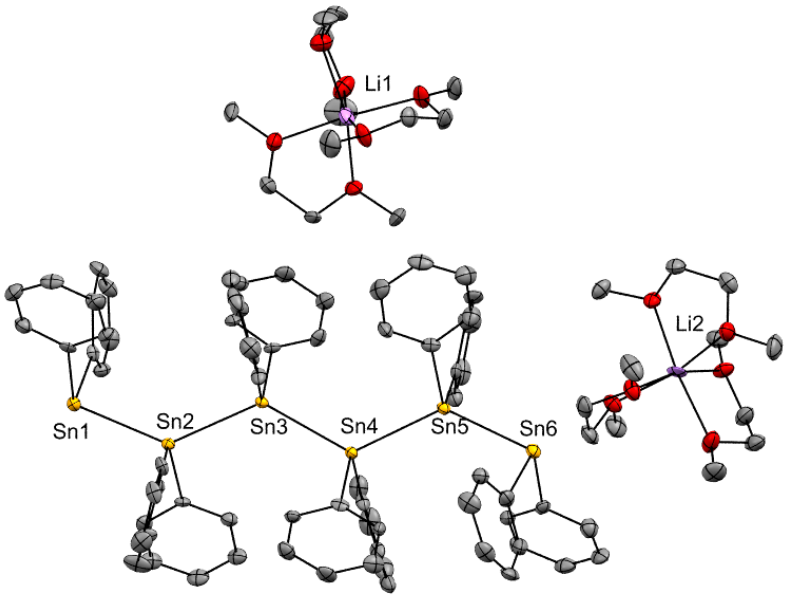


**Figure 4.12** Molecular structure of **$[Ph_{12}Sn_6]^{2-}$ $[Li{\cdot}(DME)_3]_2^+$.** Hydrogens are omitted for clarity. Ellipsoids shown at a probability of 30%. Selected bond lengths [Å] and angles [°]: Sn1-C1 2.225(9), Sn1-Sn2 2.8763(9), Sn1-C7 2.210(9), Sn2-Sn3 2.8232(9), Sn2-C13 2.201(9), Sn2-C19 2.184(9), Sn3-Sn4 2.8207(9), Sn3-C25 2.188(9), Sn3-C31 2.157(9), Sn4-C37 2.174(9), Sn4-C43 2.178(9), Sn4-Sn5 2.8280(9), Sn6-Sn5 2.8791(9), C49-Sn5 2.165(9), C55-Sn5 2.179(9) Sn6-C61 2.217(9), Sn6-C67 2.213(9); Sn1-Sn2-Sn3 133.53(3), Sn1-Sn2-C13 106.5(2), Sn1-Sn2-C19 106.3(2), Sn3-Sn2-C13 102.9(2), Sn3-Sn2-C19 102.4(2),Sn2-Sn3-Sn4 127.02(3), Sn2-Sn3-C25 103.7(2), Sn2-Sn3-C31 107.5(2), Sn3-Sn4-C37 106.1(2), Sn3-Sn4-C43 109.9(2), Sn3-Sn4-Sn5 125.31(3), Sn4-Sn5-Sn6 129.01(3), Sn5-Sn6-C61 101.6(2), Sn5-Sn6-C67 98.1(2).

In the case of using potassium in DME a dark red mother liquor and red-greenish crystals formed at room temperature. Via X-ray structure analysis, initially $[Ph_{12}Sn_6]^{2-}$ $[K(DME)_3]_2^+$ was observed. The same results were gained with Na, Rb or Cs in DME under otherwise identical reaction conditions (Scheme 4.15). To the supernatant 15cr5 (Na) or 18cr6 (K, Rb, Cs) was added and the reaction mixture was stored at -30°C. After three days orange crystals of $[Ph_8Sn_4]^{2-}$ $[K\ 18cr6)_2]_2^+$ formed. Notably, when crystals of $[Ph_{12}Sn_6]^{2-}$ $[K(DME)_3]_2^+$ were stored in contact with the supernatant at room temperature, the violet product is completely consumed after several days and is replaced by orange crystals of $[Ph_8Sn_4]^{2-}$ $[K(DME)_3]_2^+$. Attempts to investigate the supernatant by NMR spectroscopy did no diagnostic peaks of dianions or other tin containing species.

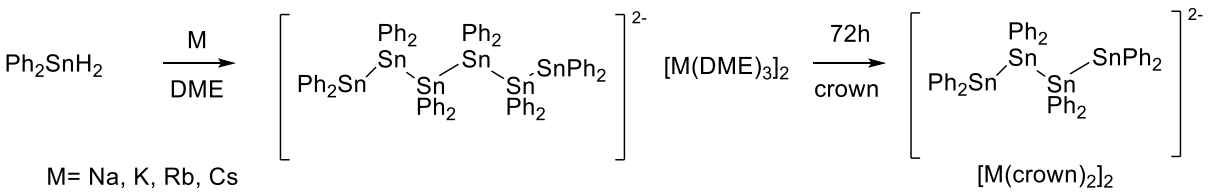


**Scheme 4.15** Formation of **$[Ph_{12}Sn_6]^{2-}$ $[M\ (crown)_2]_2^+$** and further to **$[Ph_8Sn_4]^{2-}$ $[M\ (crown)_2]_2^+$**

### 4.1.3 Formation of reduced Polystannanes from $Ph_2SnH_2$ and alkali metals

The reaction of diphenyltin dihydride with lithium in THF yields an intensively bright red solution from which brownish-purple, almost black, crystals precipitate upon cooling to -30°C. Single crystal X-ray diffraction analysis reveals a unique polymeric arrangement in the solid state, in which the tin chains adopt a strictly trans-oriented chain. Four polymer chains form a square shaped columnar cavity which is occupied by lithium cations that are tetrahedrally coordinated by four THF molecules. The overall stoichiometry adds to a tin:lithium ratio of 3:1. The remaining voids are filled by uncoordinated THF molecules.

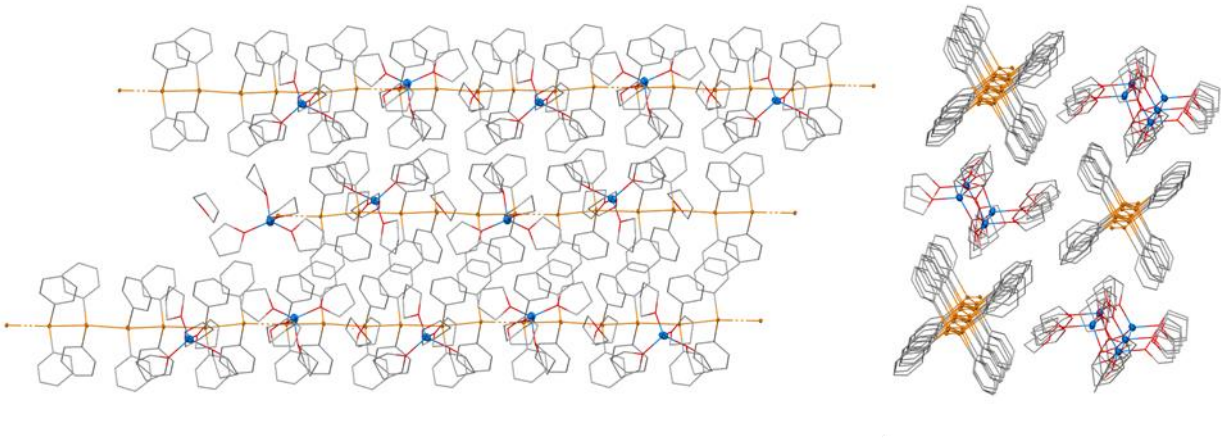

**Figure 4.13** Molecular structure of **poly{[$Ph_2Sn$]$_9$[Li·(THF)]$_3$}.** Hydrogens are omitted for clarity. Ellipsoids shown at a probability of 30%. Carbon and oxygen atoms are depicted as sticks.

Similarly, the reaction between $Ph_2SnH_2$ and sodium in THF yielded an intensively red reaction mixture. As storage at room temperature did not yield crystals suitable for X-ray diffraction analysis, the reaction mixture was cooled to -30°C, whereupon dark brown, almost black needles of poly{[$Ph_2Sn$]$_4$[Na·(15cr5)THF]} precipitated. In contrast to the lithium containing compound a ratio of 4:1 between tin and sodium is found in this compound.

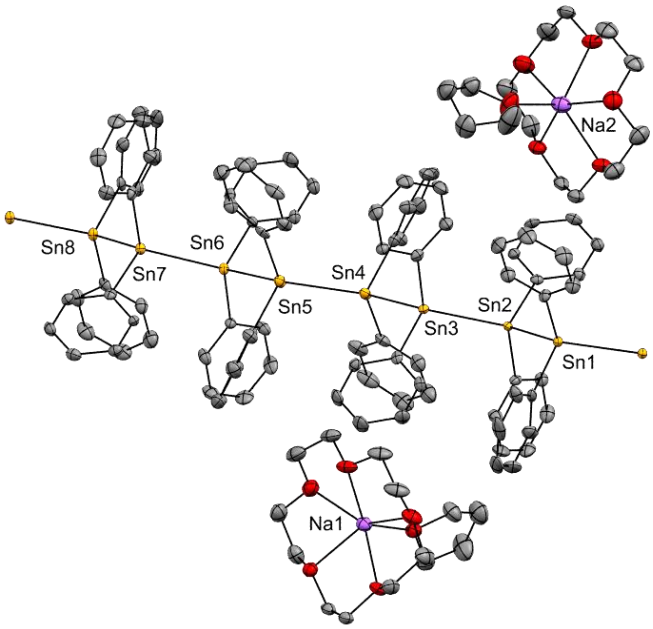


**Figure 4.14** Molecular structure of **poly $Ph_2Sn[Na{\cdot}(15cr5)]_2^+$.** Hydrogens are omitted for clarity. Ellipsoids shown at a probability of 30%. Selected bond lengths [Å] and angles [°]: Sn1-Sn2 2.8199(7), Sn1-C1 2.164(4), Sn1-C7 2.167(4), Sn1-Sn12.8067(6), Sn2-Sn3 2.8299(6), Sn2-C13 2.171(4), Sn2-C19 2.179(4), Sn3-Sn4 2.8762(7), Sn3-C25 2.182(4), Sn3-C31 2.179(4), Sn4-Sn5 2.9189(7), Sn4-C37 2.198(5), Sn4-C43 2.211(4), Sn5-Sn6 2.8670(7), Sn5-C49 2.196(4), Sn5-C55 2.196(5), Sn6-Sn7 2.8268(6), Sn6-C61 2.185(4), Sn6-C67 2.183(4), Sn7-Sn8 2.8182(7), Sn7-C73 2.187(4), Sn7-C79 2.176(5), Sn8-C85 2.176(5), Sn8-C91 2.172(4), Sn8-Sn8 2.8005(6); Sn2-Sn1-Sn1 128.70(2), Sn1-Sn2-Sn3 127.61(2), Sn2-Sn3-Sn4 133.65(2), Sn3-Sn4-Sn5 146.56(2), Sn4-Sn5-Sn6 144.37(2), Sn5-Sn6-Sn7 132.74(2), Sn6-Sn7-Sn8 126.81(2), Sn7-Sn8-Sn8 127.23(2).

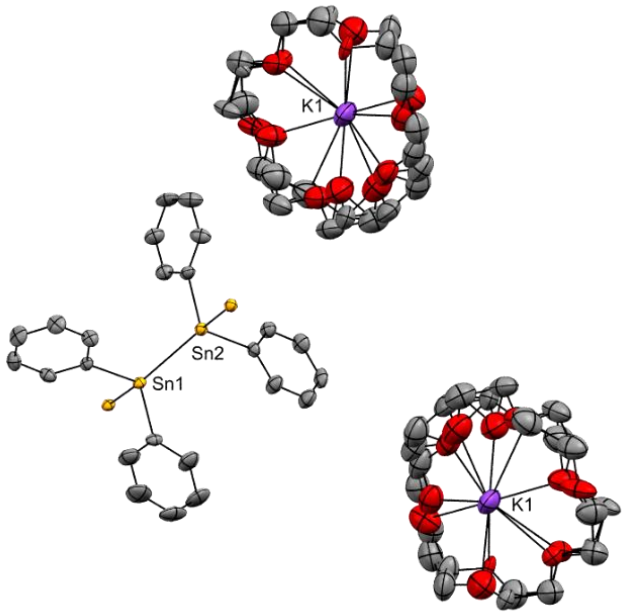


**Figure 4.15** Molecular structure of **poly $Ph_2Sn[K{\cdot}(18cr6)]_2^+$.** Hydrogens are omitted for clarity. Ellipsoids shown at a probability of 30%. Selected bond lengths [Å] and angles [°]:Sn1-Sn2 2.8302(5), Sn1-Sn1 2.8316(5), Sn2-Sn2, 2.8275(5), C19-Sn2 2.174(4), C13-Sn2 2.175(4), C7-Sn1 2.179(4), C1-Sn1 2.170(4). C2-C1-Sn1 122.2(3), C6-C1-Sn1 122.0(3), C8-C7-Sn1 121.3(3), C12-C7-Sn1 121.1(3), C14-C13-Sn2 120.9(3), C18-C13-Sn2 122.7(3) C20-C19-Sn2 121.5(3), C24-C19-Sn2 121.0(3), C1-Sn1-C7 101.7(2), C1-Sn1-Sn2 105.1(1), C1-Sn1-Sn1 104.6(1), C7-Sn1-Sn2 104.7(1), C7-Sn1-Sn1 104.2(1), Sn2-Sn1-Sn1 132.82(1), C13-Sn2-C19 101.4(2), C13-Sn2-Sn1 103.9(1), C13-Sn2-Sn2 105.2(1), C19-Sn2-Sn1 104.9(1), C19-Sn2-Sn2 104.6(1), Sn1-Sn2-Sn2 132.85(1).

Similarly, a 4:1 ratio between tin and potassium and rubidium is obtained, when diphenyltin dihydride was dissolved in benzene and 0.5 equivalents of 18cr6 and 0.25 equivalents of potassium or rubidium were added the the reaction mixture. The addition of the alkali metals result in immediate gas evolution while the surface of the metals adopt a dark red color. After ca. 12-24 hours, black needles start to grow from the metal surface. These were confirmed to to be crystals of the potassium and rubidium containing reduces polystannanes poly{[$Ph_2Sn]_4[M{\cdot}(18cr6)_2]$}, M=K, Rb. Extended reaction times lead to a slow consumption of the polymeric material, whereupon the previously described dianions $[Ph_2Sn]_6[M(18cr6)_2]$, M=K, Rb form.

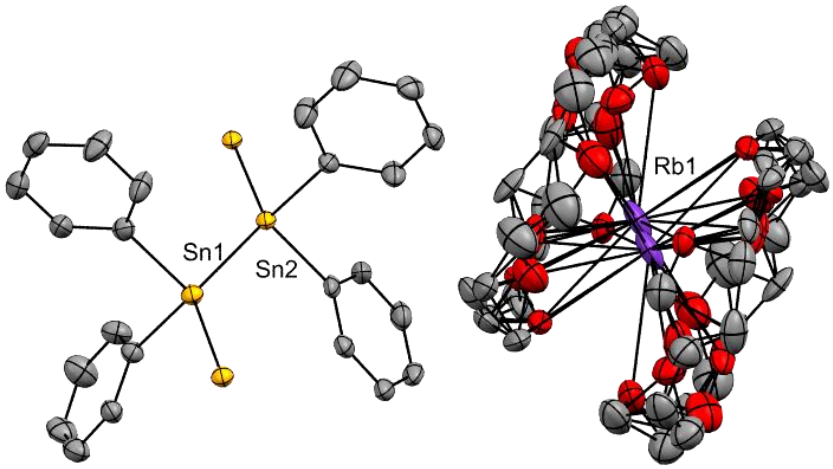


**Figure 4.16** Molecular structure of **poly $Ph_2Sn[Rb\ (18cr6)]_2^+$**. Hydrogens are omitted for clarity. Ellipsoids shown at a probability of 30%. Selected bond lengths [Å] and angles [°]: Sn1-C1 2.188(5), Sn1-Sn2 2.8287(6), Sn1-C7 2.179(7), Sn1-Sn1 2.8235(7), Sn2-C13 2.185(7), Sn2-C19 2.185(5), Sn2-Sn2 2.8262(7); C1-Sn1-Sn2 104.9(2), C1-Sn1-C7 101.8(2), C1-Sn1-Sn1 104.0(2), Sn2-Sn1-C7 104.9(2), Sn2-Sn1-Sn1 133.33(2), C7-Sn1-Sn1 104.1(2), Sn1-C1-C2 121.6(5), Sn1-C1-C6 120.1(4), Sn1-Sn2-C13 105.0(2), Sn1-Sn2-C19 106.8(2), Sn1-Sn2-Sn2 131.63(2), C13-Sn2-C19 102.3(2), C13-Sn2-Sn2 103.1(2), C19-Sn2-Sn2 104.6(2).

The same result was observed in the case of using potassium/rubidium/cesium in diglyme. A dark red mother liquor and red-greenish crystals formed at room temperature. Via X-ray analysis $[Ph_{12}Sn_6]^{2-}$ [M (diglyme)$_3]_2^+$ could be observed.

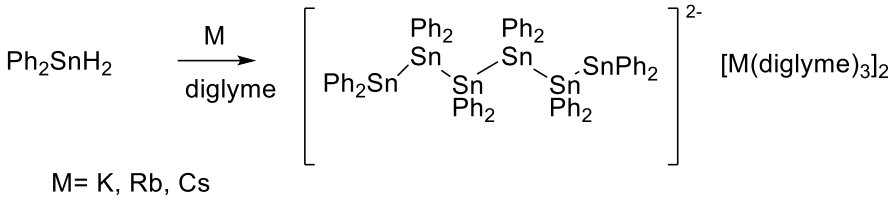


**Scheme 4.16** Formation of **$[Ph_{12}Sn_6]^{2-}$ [M (diglyme)$_3$]$_2^+$**

The $[Ph_{12}Sn_6]^{2-}$ alkali metal compounds are hardly soluble in organic solvents like ethers, crown ethers of aromatic hydrocarbons. The dianions are less stable in ethereal solution and undergo redistribution and rearrangement reactions. However, $[Ph_{12}Sn_6]^{2-}$ is soluble in acetonitrile or liquid ammonia.

When diphenyltin dihydride is reacted with cesium in diglyme. the initial reaction product is again a reduced polystannane of the composition poly{$[Ph_2Sn]_4[Cs(diglyme_3]$}.

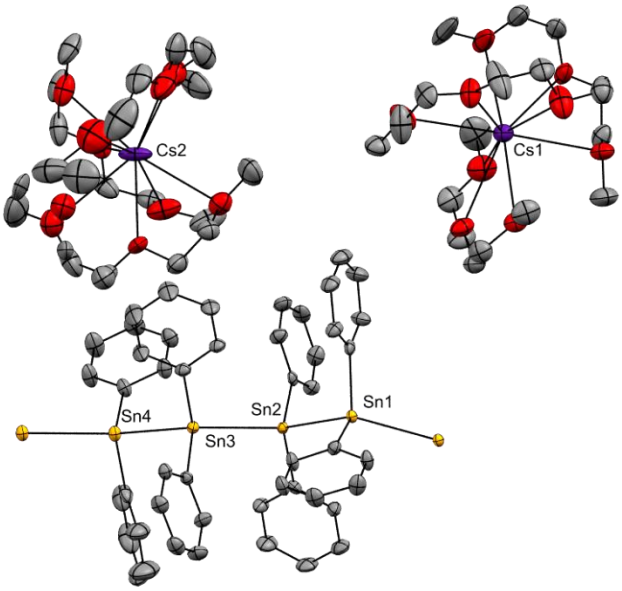


**Figure 4.17** Molecular structure of **poly Ph$_2$Sn [Cs(diglyme)$_3$]$_2^+$**. Hydrogens are omitted for clarity. Ellipsoids shown at a probability of 30%. Selected bond lengths [Å] and angles [°]:Sn1-Sn2 2.8009(6), Sn1-C1 2.159(7), Sn1-C7 2.158(5), Sn1-Sn1 2.7944(6), Sn2-Sn3 2.8233(5), Sn2-C13 2.169(5), Sn2-C19 2.172(6), Sn3-Sn4 2.8564(6), Sn3-C25 2.178(7), Sn3-C31 2.167(5), Sn4-C37 2.165(5), Sn4-C43 2.182(7), Sn4-Sn4 2.8857(5); Sn2-Sn1-C1 107.5(2), Sn2-Sn1-C7 102.1(2), Sn2-Sn1-Sn1 127.36(2), C1-Sn1-C7 106.8(2), C1-Sn1-Sn1 103.6(2), C7-Sn1-Sn1 108.1(2), Sn1-Sn2-Sn3 128.64(2), Sn1-Sn2-C13 107.7(2), Sn1-Sn2-C19 104.5(1), Sn3-Sn2-C13 105.3(2), Sn3-Sn2-C19 105.5(1), C13-Sn2-C19 102.4(2), Sn2-Sn3-Sn4 136.74(2), Sn2-Sn3-C25 102.4(2), Sn2-Sn3-C31 104.5(2), Sn4-Sn3-C25 104.1(2), Sn4-Sn3-C31 102.9(2), C25-Sn3-C31 101.6(2), Sn3-Sn4-C37 100.4(2), Sn3-Sn4-C43 104.0(2), Sn3-Sn4-Sn4 139.64(2), C37-Sn4-C43 99.8(2), C37-Sn4-Sn4 103.5(2), C43-Sn4-Sn4 103.4(2).

Finally, reaction of diphenyltin dihydride with sodium in diglyme yields the octastnnadiide $[Ph_{16}Sn_8]^{2-}$ $[Na(diglyme)_3]_2^+$.

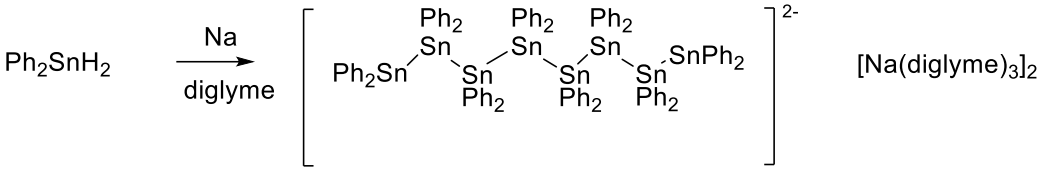


**Scheme 4.17** Formation of **$[Ph_{16}Sn_8]^{2-}$ $[Na\ (diglyme)_3]_2^+$**

The crystal structure is identical to the structure shown in Figure 4.9.

**Table 4.1.3** Overview of average bond length [Å] and angles [°] of anionic tin oligomers with different alkali metals

| | **Sn-Sn** | **Sn-C** | **Sn-Sn-Sn** |
|---|---|---|---|
| | [Å] (averg.) | [Å] (averg.) | [°] (averg.) |
| **poly $Ph_2SnLi$** | 2.8432(9) | 2.180(9) | 128.72(3) |
| **poly $Ph_2SnNa$** | 2.8413(7) | 2.183(4) | 134.06(2) |
| **poly $Ph_2SnK$** | 2.8295(5) | 2.175(4) | 132.84(1) |
| **poly $Ph_2SnRb$** | 2.8275(6) | 2.182(5) | 132.48(2) |
| **poly $Ph_2SnCs$** | 2.8321(6) | 2.172(7) | 135.01(2) |

The bond lengths of the anionic tin oligomers are all in the same range. The largest Sn-Sn bond length could be detected for the polymeric chain using lithium or sodium with 2.843(9) Å and 2.8413(7) Å. The Sn-Sn bond length of the other polymeric chains of K, Rb or Cs are nearly the same. The Sn-C bond distance for the polymeric chain using potassium or cesium is the shortest with a length of 2.172(7) Å. For all compounds the alkali metals clearly don't have much effect on the Sn-Sn-Sn angles, except for the example using lithium, where the angle difference is about 5° compared to the others.

# 5 Summary

The aim of this master thesis was to study the coupling reactions and the formation of anionic tin oligomers. In order to isolate the intermediate building blocks, reactions of $Ph_2SnH_2$ with alkaline metal derivates like methyllithium, *n*-Butyllithium or LiHMDS in different solvents, were executed and controlled by heteronuclear NMR spectroscopy and X-ray crystallography. Successfully, crystal structures of the monomeric $Ph_2SnH^-$ species and the dimeric $Ph_2SnSnPh_2H^-$ could be isolated. These results explain the formation of the anionic tin chains and how they grow, as well as any rearrangement reactions, after some time, from $[Ph_{12}Sn_6]^{2-}$ to $[Ph_8Sn_4]^{2-}$. During these reactions series another interesting compound could be isolated and observed, a neutral polystannane -$[Ph_2Sn]$-.
Furthermore, the formation of the anionic tin chains was detected, using different alkaline metals like lithium, sodium, potassium, rubidium or caesium. Crystal structures were determined and discussed how the alkaline metals affect the bond length and angles.

# 6 Synthesis

All manipulations were carried out in dry solvents using inert standard tube Schlenk techniques under a nitrogen atmosphere or in a nitrogen flushed Glovebox UNILAB supplied by M.Braun. The dried and deoxygenated solvents were obtained from an Innovative Technology solvent drying system. All other chemicals from commercial sources were used as purchased from chemical supply. For the NMR analysis $C_6D_6$ degassed, using the freeze pump method, was used as a solvent. $^{1}H$ (300.22 MHz) ,$^{13}C$ (75.5 MHz) and $^{119}Sn$ (111.92MHz) NMR spectra were recorded on a Varian Mercury 300 MHz spectrometer. Spectra were referenced to solvent residual signals. All UV/VIS measurements were performed with Agilent Technologies Cary-60. Melting point measurements were determined with a stuart SMP50 automatic melting point instrument.

For single crystal X-ray diffractometry all suitable crystals were covered with a layer of silicone oil. For single crystal X-ray diffractometry all suitable crystals were covered with a layer of silicone oil. A single crystal was selected, mounted on a glass rod on a copper pin, and placed in the cold $N_2$ stream provided by an Oxford Cryosystems cryometer (T=100 K). XRD data collection was performed on a Bruker APEX II diffractometer with use of Mo Kα radiation (λ= 0.71073 Å) from an IμS microsource and a CCD area detector. Empirical absorption corrections were applied using SADABS. [2] [3] The structures were solved with use of either direct methods or the Patterson option in SHELXS and refined by the full-matrix least-squares procedures in SHELXL. [4] [5] The space group assignments and structural solutions were evaluated using PLATON. [6] [7] All non-hydrogen atoms were refined anisotropically. All hydrogen atoms were placed in calculated positions corresponding to standard bond lengths and angles using riding models.

## [1] Synthesis of $Ph_2SnCl_2$

$Ph_3SnCl$ (100 g, 259 mmol, 2.0 eq) and $SnCl_4$ (33.8 g, 130 mmol, 1.0 eq) were mixed in a 500 mL Schlenk flask and heated in a 140°C oil bath for 3 h. Then the reaction was allowed to cool to room temperature overnight. A colorless precipitate formed. The conversion was controlled by NMR in $CDCl_3$. The solid was extracted with 150 mL degassed *n*-heptane, the residual grey solid was separated via filter canula. The filtrate was cooled to -30°C to a colorless solid. Heptane was removed via extraction. The product was dried on vacuum.

Yield: 116.9 g (87%). $^1H$ (300.22 MHz, $C_6D_6$): δ 7.83-7.80 (m, 4 H; 4x $H^{Ar}$), 7.32-7.26 (m, 6H; 6x$H^{Ar}$) ppm. $^{119}Sn$ NMR (111.92 MHz, $C_6D_6$): δ -27.80 ppm.

## [2] Synthesis of $Ph_2SnH_2$

Fine powdered $LiAlH_4$ (1.84 g, 49 mmol, 0.84 eq) in 200 mL degassed $Et_2O$ formed to a brownish suspension. To that $Ph_2SnCl_2$ (20.1 g, 58 mmol, 1.0 eq) was added in portions at 0°C. After 3h the reaction was quenched via filter canula in 100 mL degassed $H_2SO_4$ (0.5 M). The organic phase is then quenched 2x in 150 mL degassed saturated Potassium tartrate solution and dried with $Na_2SO_4$ and filtered. The solvent was removed and the product was dried on vacuum. A light-yellow oil was observed.

Yield: 11.1 g (69%). $^1H$ NMR (300.22 MHz, $C_6D_6$): δ 7.37 (s, $^3J_{H,Sn}$ = 54.8 Hz, 4 H; 4x $H^{Ar}$), 7.07-7.09 (m, 6 H; 6x $H^{Ar}$), 6.07 (s, $^1J_{H,119Sn}$ = 1922.59 Hz, 2 H; $SnH_2$) ppm. $^{119}Sn$ NMR (111.92 MHz, $C_6D_6$): δ -233.50 ($^1J_{Sn,H}$ = 1922.59 Hz) ppm.

## [3] Reaction of $Ph_2SnH_2$ with MeLi in THF

In a 20 mL glass vial $Ph_2SnH_2$ (275 mg, 1.0 mmol, 0.5 eq) was dissolved in 10 mL THF. To the colorless solution $Ch_3Li$ 1.6M (0.69 mL, 1.1 mmol,1.1 eq) was added. An orange-red solution formed, no precipitate. The reaction did not work.

## [4] Reaction of $Ph_2SnH_2$ with MeLi in THF

In a 20 mL glass vial $Ph_2SnH_2$ (275 mg, 1.0 mmol, 1.0 eq) was dissolved in 10 mL THF. To the light-yellow solution $CH_3Li$ 1.6M (0.63 mL, 1.1 mmol,1.0 eq) was added. The reaction turned cloudy yellow. After two days a black precipitate formed in a yellow-greenish solution. The reaction did not work.

### [5] Reaction of $Ph_2SnH_2$ with MeLi and 12cr4 in THF

In a 20 mL glass vial $Ph_2SnH_2$ (275 mg, 1.0 mmol, 1.0 eq) was dissolved in 10 mL THF. To the light-yellow solution $CH_3Li$ 1.6M (0.06 mL, 1.0 mmol, 1.0 eq) was added and 12cr4 (352 mg, 2.0 mmol, 2.0 eq). The reaction turned cloudy dark yellow. After two days black precipitate formed in a yellow greenish solution. The reaction did not work.

### [6] Synthesis of $[Ph_{10}Sn_6]^{2-}$ $[Li{\cdot}(12cr4)_2]_2^+$

In 20 mL glass vial $Ph_2SnH_2$ (275 mg, 1.0 mmol, 1.0 eq) was dissolved in 10 mL THF. To the light-yellow solution $CH_3Li$ 1.6M (0.06 mL, 0.1 mmol, 0.1 eq) was added and 12cr4 (352 mg, 2.0 mmol, 2.0 eq). The reaction turned to a clear dark-orange solution. Suitable for NMR spectroscopy.

UV-VIS ($CH_3CN$) λ= 287 nm. $^1$H NMR (300.22 MHz, $C_6D_6$) δ 7.36-7.18 (m, 4 $H^{Ar}$, overlay with solvent residual signal), 7.04-6.99 (m, $H^{Ar}$, overlay with solvent residual signal) ppm. $^{119}$Sn NMR (111.92 MHz, $C_6D_6$) δ -207.64 ppm.

### [7] Synthesis of octaphenyl tetrastanna-1,4-diides $(Sn_4Ph_8)Li_2$ in THF

In a 20 mL glass vial $Ph_2SnH_2$ (275 mg, 1.0 mmol, 1.0 eq) was dissolved in 10 mL DME. To the light-yellow solution $CH_3Li$ 1.6M (0.16 mL, 0.25 mmol, 0.25 eq) was added and 12cr4 (356 mg, 2.1 mmol, 2.1 eq). The reaction first turned yellow, then dark red and was put in the fridge overnight. In the red mother liquor red fine precipitate and colorless fine crystals formed. After two weeks, black-violet crystals formed. Suitable for X-ray diffraction.

### [8] Reaction of $Ph_2SnH_2$ with MeLi in THF

In a 20 mL glass vial $Ph_2SnH_2$ (140 mg, 0.51 mmol, 3.0 eq) was dissolved in 10 mL THF. To the light-yellow solution $CH_3Li$ 1.6M (0.11 mL, 0.17 mmol, 1.0 eq) was added and 12cr4 (356 mg, 2.1 mmol, 2.1 eq). The reaction turned to a clear yellow solution. Orange crystals suitable for single crystal X-ray diffraction were obtained by recrystallisation.

$^1$H NMR (300.22 MHz, $C_6D_6$): δ 7.70-6.85 (m, $H^{Ar}$, overlay with solvent residual signal), 0.95 (t, 2 H; $CH_2$) ppm. $^{119}$Sn NMR (111.92 MHz, $C_6D_6$) δ -0.62 [$Ph_2SnMe_2$], -29.19, -60.33, 88.83, -108.91 [$Ph_3SnLi$], -181.78 [$Ph_2HSnSnPh_2Li$], -188.33 [$Ph_2HSnSnPh_2Li$] ppm.

### [9] Reaction of $Ph_2SnH_2$ and MeLi in THF

In a 20 mL glass vial $CH_3Li$ 1.6M (0.08 mL, 0.13 mmol, 1.0 eq) was dissolved in 10 mL THF. $Ph_2SnH_2$ (140 mg, 0.51 mmol, 4.0 eq) was added dropwise, the reaction turned intense yellow. After two weeks a black precipitate (Sn) formed. The reaction did not work.

### [10] Reaction of $Ph_2SnH_2$ with MeLi and 12cr4 in diglyme

In a 20 mL glass vial $Ph_2SnH_2$ (275 mg, 1.0 mmol, 1.0 eq) was dissolved in 10 mL diglyme. To the light-yellow solution $CH_3Li$ 1.6M (0.69 mL, 1.1 mmol, 1.0 eq) was added and 12cr4 (356 mg, 2.0 mmol, 2.0 eq). The reaction turned intense yellow and later cloudy. Colorless blackish precipitate formed, in a yellow greenish mother liquor. The reaction did not work.

### [11] Reaction of $Ph_2SnH_2$ with MeLi in diglyme

In a 20 mL glass vial $Ph_2SnH_2$ (275 mg, 1.0 mmol, 1.0 eq) was dissolved in 10 mL diglyme. To the light-yellow solution $CH_3Li$ 1.6M (0.69 mL, 1.1 mmol, 1.1 eq) was added and 12cr4 (352 mg, 2.0 mmol, 2.0 eq). The reaction turned cloudy yellow. Colorless blackish precipitate formed, in a yellow greenish mother liquor. The reaction did not work.

### [12] Reaction of $Ph_2SnH_2$ with MeLi and 12cr4 in DME

In a 20 mL glass vial $Ph_2SnH_2$ (275 mg, 1.0 mmol, 1.0 eq) was dissolved in 10 mL DME. To the light-yellow solution $CH_3Li$ 1.6M (0.69 mL, 1.1 mmol, 1.0 eq) was added and 12cr4 (356 mg, 2.0 mmol, 2.0 eq). The reaction turned intense yellow and later also cloudy. Colorless blackish precipitate formed, which was removed by centrifugation. An NMR spectrum could be observed of the mother liquor.

$^1H$ NMR (300.22 MHz, $C_6D_6$): δ 8.04-8.02 (m, $H^{Ar}$, overlay with solvent residual signal), 7.87-7.84 (m, $H^{Ar}$), 7.13-6-67 (s, $^1J_{H,119Sn}$ = 53.35 Hz, H; SnH) ppm. $^{119}Sn$ NMR (111.92 MHz, $C_6D_6$): δ -29.47, -109.06 [$Ph_3SnLi$], -182.47 (broad) [$Ph_2HSnSnPh_2Li$] ($^1J_{Sn,H}$ = 53.35 Hz), -194.41 [$Ph_2HSnSnPh_2Li$] ppm.

### [13] Reaction of $Ph_2SnH_2$ with MeLi, 12cr4 in DME

In a 20mL glass vial $Ph_2SnH_2$ (138 mg, 0.5 mmol, 1.0 eq) was dissolved in 10 mL DME. To the light-yellow solution $CH_3Li$ 1.6M (0.31 mL, 0.5 mmol, 1.0 eq) was added and 12cr4 (179 mg,

1.0 mmol, 2.0 eq). A colorless precipitate formed in a light-yellow mother liquor. The next day an additional equivalent $Ph_2SnH_2$ (138 mg, 0.5 mmol, 1.0 eq) is added which reacts with the colorless precipitate, blistering could be detected. The reaction turned dark yellow. The next day 12cr4 (179 mg, 1.0 mmol, 2.0 eq) is added, the reaction immediately turned intense red. Orange crystals suitable for single crystal X-ray diffraction were obtained by recrystallisation.

$^1$H NMR (300.22 MHz, $C_6D_6$): δ 7.83-7.81 (d), 7.67-7.64 (d), 6.07 (m, $^1J_{H,119Sn}$ = 56.22 Hz, H; SnH, overlay with solvent residual signal), 0.95 (t, 2 H; $CH_2$) ppm. $^{119}$Sn NMR (111.92 MHz, $C_6D_6$) δ 0.60 [$Ph_2SnMe_2$], -29.04, -108.62 [$Ph_3SnLi$], -180.32 [$Ph_2HSn$] (broad) ($^1J_{Sn,H}$ = 56.22 Hz) ppm.

### [14] Reaction of $Ph_2SnH_2$ with LiH and 12cr4 in DME

In a 20 mL glass vial $Ph_2SnH_2$ (275 mg, 1.0 mmol, 1.0 eq) was dissolved in 10 mL DME. To the light-yellow solution LiH (8.0 mg, 1.0 mmol, 1.0 eq) was added and 12cr4 (356 mg, 2.0 mmol, 2.0 eq). A colorless precipitate in a yellow mother liquor formed.

### [15] Reaction of $Ph_2SnH_2$ with MeLi and 12cr4 in DME

In a 20 mL glass vial $Ph_2SnH_2$ (140 mg, 0.51 mmol, 3.0 eq) was dissolved in 10 mL DME. To the light-yellow solution $CH_3Li$ 1.6M (0.11 mL, 0.17 mmol, 1.0 eq) was added and 12cr4 (136 mg, 0.77 mmol, 3.5 eq). The reaction starts blistering and turned intense yellow.

### [16] Reaction of $Ph_2SnH_2$ with MeLi and 12cr4 in DME

In a 20 mL glass vial $Ph_2SnH_2$ (140 mg, 0.51 mmol, 4.0 eq) was dissolved in 10 mL DME. To the light-yellow solution $CH_3Li$ 1.6M (0.07 mL, 0.13 mmol, 1.0 eq) was added and 12cr4 (136 mg, 0.77 mmol, 4.5 eq). A colorless precipitate formed in a light-yellow precipitate.

### [17] Reaction of $Ph_2SnH_2$ with MeLi and 12cr4 in DME

In a 20 mL glass vial $Ph_2SnH_2$ (140 mg, 0.51 mmol, 8.0 eq) was dissolved in 10 mL DME. To the light-yellow solution $CH_3Li$ 1.6M (0.04 mL, 0.06 mmol, 1.0 eq) was added and 12cr4 (136 mg, 0.77 mmol, 8.5 eq). The reaction turned to a clear dark-orange solution. The next day a colorless precipitate formed. An NMR spectrum could be observed.

$^{1}$H NMR (300.22 MHz, $C_6D_6$): δ 7.64-6.78 (m, $H^{Ar}$, overlay with solvent residual signal), 0.94 (t, 2 H; $CH_2$) ppm. $^{119}$Sn NMR (111.92 MHz, $C_6D_6$) δ -28.89, -59.77 [$Ph_2SnMe_2$], -128.26 [$Ph_4Sn$] ppm.

### [18] Synthesis of octaphenyl tetrastanna-1,4-diides $(Sn_4Ph_8)Li_2$ in DME

In a 20 mL glass vial $CH_3Li$ 1.6M (0.64 mL, 1.0 mmol, 2.0 eq) was dissolved in 10 mL DME. To that 12cr4 (181 mg, 1.0 mmol, 2.0 eq) was added. A cloudy colorless suspension formed. $Ph_2SnH_2$ (140 mg, 0.51 mmol, 1.0 eq) was added dropwise, blistering started immediately. NMR spectrum could be observed.

$^{1}$H NMR (300.22 MHz, $C_6D_6$): δ 7.86-7.84 (d, $H^{Ar}$), 7.68-7.66 (d, $H^{Ar}$), 6.95-6.85 (m, $^{1}J_{H,119Sn}$ = 55.78 Hz, H; SnH), 0.95 (t, 2 H; $CH_2$) ppm. $^{119}$Sn NMR (111.92 MHz, $C_6D_6$) δ -0.34 [$Ph_2SnMe_2$], -108.81 [$Ph_3SnLi$], -180.66 [$Ph_2HSnSnPh_2Li$] ( $^{1}J_{Sn,H}$ = 55.78 Hz,  SnH) ppm.

### [19] Reaction of $Ph_2SnH_2$ with MeLi and 12cr4 in DME

In a 20 mL glass vial $CH_3Li$ 1.6M (0.3 mL, 0.51 mmol, 1.0 eq) was dissolved in 10 mL DME. Additionally, 12cr4 (181 mg, 1.0 mmol, 2.0 eq) was added under stirring. $Ph_2SnH_2$ (140 mg, 0.51 mmol, 1.0 eq) was added dropwise, a light-yellow solution formed. A fine yellow precipitate formed in a orange mother liquor. ($^{119}$Sn-NMR: no signals could be observed)

### [20] Reaction of $Ph_2SnH_2$, MeLi, 12cr4 and DME in $Et_2O$

In a 20 mL glass vial $CH_3Li$ 1.6M (0.6 mL, 1.0 mmol, 2.0 eq) was dissolved in 10 mL $Et_2O$. 12cr4 (181 mg, 1.0 mmol, 2.0 eq) and DME (100 mg, 1.0 mmol, 2.0 eq) were added under stirring. $Ph_2SnH_2$ (140 mg, 0.51 mmol, 1.0 eq) was added dropwise, intense blistering started. The reaction turned cloudy yellow and a colorless precipitate formed. After a day the precipitate is recrystallized in DME and the $Et_2O$ phase is removed. Two weeks later fine orange crystals formed. Suitable for NMR spectroscopy.

$^{119}$Sn NMR (111.92 MHz, $C_6D_6$): δ -181.70 [$Ph_2HSnSnPh_2Li$] ppm.

### [21] Reaction of $Ph_2SnH_2$ with MeLi and 12cr4 in $Et_2O$

In a 20 mL glass vial $CH_3Li$ 1.6M (0.7 mL, 1.1 mmol, 2.2 eq) was dissolved in 10 mL $Et_2O$. Additionally, 12cr4 (181 mg, 1.0 mmol, 2.0 eq) was added. To that colorless cloudy suspension

$Ph_2SnH_2$ (140 mg, 0.51 mmol, 1.0 eq) was added dropwise, intense blistering started immediately. After one hour a yellow oily precipitate formed in a colorless mother liquor. The reaction was put in the fridge overnight. A yellow fine precipitate formed. By NMR and X-ray analysis it could be detected that the educt $Ph_2SnH_2$ formed again and $^{cy}[Ph_{10}Sn_6]^{2-}$ $[Li.4THF]^{2+}$, so the reaction failed.

## [22] Reaction of $Ph_2SnH_2$ with MeLi and 12cr4 in $Et_2O$

In a 20 mL glass vial $CH_3Li$ 1.6M (0.7 mL, 1.1 mmol, 2.2 eq) was dissolved in 10 mL $Et_2O$. To that 12cr4 (181mg, 1.0 mmol, 2.0 eq) was added. To that colorless cloudy suspension $Ph_2SnH_2$ (140 mg, 0.51mmol, 1.0 eq) was added dropwise, blistering started immediately. After one hour a yellow oily precipitate formed in a colorless mother liquor. The reaction was put in the fridge overnight. An NMR spectrum could be observed from the precipitate. Colorless crystals suitable for single crystal X-ray diffraction were obtained by recrystallisation.

$^1H$ NMR (300.22 MHz, $C_6D_6$): δ 7.68-7.62 (m, $H^{Ar}$), 7.47-7.45 (m, $H^{Ar}$), 6.77-6.67 (m, $^1J_{H,119Sn}$ = 54.77 Hz, H; SnH) ppm. $^{119}Sn$ NMR (111.92 MHz, $C_6D_6$) δ -178.28 $[Ph_2SnH^-]$ ( $^1J_{Sn,H}$ = 54.77 Hz, SnH) ppm.

## [23] Reaction of $Ph_2SnH_2$ with MeLi and 12cr4 yielding $[Ph_2SnH^-]$

In a 20 mL glass vial $CH_3Li$ 1.6M (0.7 mL, 1.1 mmol, 2.2 eq) was dissolved in 10 mL $Et_2O$. Additionally, 12cr4 (181 mg, 1.0 mmol, 2.0 eq) was added. To that colorless cloudy suspension $Ph_2SnH_2$ (140 mg, 0.51 mmol, 1.0 eq) was added dropwise, blistering started immediately. After one hour a yellow oily precipitate formed in a colorless mother liquor. The precipitate is removed from the mother liquor and put in the fridge overnight. After one day fine orange crystals could be observed. Suitable for X-ray diffraction. The precipitate was dissolved in DME for crystallation and put in the fridge. Colorless crystals were observed, X-ray spectroscopy showed that $Ph_2SnH^-$ formed.

## [24] Reaction of $Ph_2SnH_2$ with MeLi and DME in $Et_2O$

In a 20 mL glass vial $CH_3Li$ 1.6M (0.7 mL, 1.1 mmol, 2.2 eq) was dissolved in 10 mL $Et_2O$. To that DME (157 mg, 3.4 mmol, 6.7 eq) was added under stirring, a colorless cloudy reaction formed. $Ph_2SnH_2$ (140 mg, 0.51 mmol, 1.0 eq) was added dropwise, the reaction turned cloudier. After a day a colorless precipitate formed in a clear light-yellow solution. Suitable for NMR spectroscopy.

$^{1}$H NMR (300.22 MHz, $C_6D_6$): δ 7.67-7.66 (m, $H^{Ar}$), 7.29-7.26 (m, $H^{Ar}$), 6.93-6.81 (m, $^{1}J_{H,119Sn}$ = 53.30 Hz, H; SnH), 0.96 (t, 2 H; $CH_2$) ppm. $^{119}$Sn NMR (111.92 MHz, $C_6D_6$) δ -0.28 [$Ph_2SnMe_2$], -29.27, -106.24 [$Ph_3SnH$]( $^{1}J_{Sn,H}$ = 53.30 Hz, SnH) ppm.

### [25] Reaction of $Ph_2SnH_2$ with MeLi and diglyme in $Et_2O$

In a 20 mL glass vial $CH_3Li$ 1.6M (0.7 mL, 1.1 mmol, 2.2 eq) was dissolved in 10 mL $Et_2O$. To that diglyme (141 mg, 1.1 mmol, 2.2 eq) was added under stirring, a colorless cloudy reaction formed. $Ph_2SnH_2$ (140 mg, 0.51 mmol, 1.0 eq) was added dropwise, intense blistering could be detected. The reaction turned light-yellow and cloudier. A yellow oily precipitate formed. Suitable for NMR spectroscopy.

### [26] Reaction of $Ph_2SnH_2$ with n-BuLi and 12cr4 yielding octaphenyl tetrastanna-1,4-diides $(Sn_4Ph_8)Li_2$ and tetraphenyl distanna-1,2-diides $(Sn_2Ph_4)Li_2$

In a 20 mL glass vial n-BuLi 2.5M (0.45 mL, 1.1 mmol, 2.2 eq) was dissolved in 10 mL $Et_2O$. To that 12cr4 (181mg, 1.0 mmol, 2.0 eq) was added. The reaction was stirred for a while. To that colorless cloudy suspension $Ph_2SnH_2$ (140 mg, 0.51mmol, 1.0 eq) was added dropwise, blistering started immediately. After one hour a yellow oily precipitate formed in a colorless mother liquor. The reaction is put in the fridge overnight. After two weeks orange fine crystals formed in the clear colorless mother liquor. Suitable for X-ray diffraction.

### [27] Reaction of $Ph_2SnH_2$, MeLi and 12cr4 in benzene

In a 20 mL glass vial $CH_3Li$ 1.6M (0.6 mL, 1.0 mmol, 2.0e q) was dissolved in 10 mL benzene. Additionally, 12cr4 (181 mg, 1.0 mmol, 2.0 eq) was added under stirring. $Ph_2SnH_2$ (140 mg, 0.51 mmol, 1.0 eq) was added dropwise, intense blistering started. A yellow-brownish oily precipitate formed in a clear mother liquor. Ten days later fine colorless crystals formed ($Ph_2SnH^-$). Suitable for X-ray diffraction.

$^{1}$H NMR (300.22 MHz, $C_6D_6$): δ 7.99-7.97 (m, $H^{Ar}$), 7.42-6.94 (m, $H^{Ar}$, overlay with solvent residual signal), 6.40-6.37 (m, $^{1}J_{H,119Sn}$ = 49.44 Hz, H; SnH) ppm. $^{119}$Sn NMR (111.92 MHz, $C_6D_6$): δ -108.95 (broad) [$Ph_3SnLi$], -181.70 [$Ph_2HSnSnPh_2Li$] ( $^{1}J_{Sn,H}$ = 49.44 Hz, SnH) ppm.

### [28] Reaction of $Ph_2SnH_2$, MeLi and 12cr4 in benzene

In a 20 mL glass vial $CH_3Li$ 1.6M (0.6 mL, 1.0 mmol, 2.0 eq) was dissolved in 10 mL benzene. Additionally, 12cr4 (181 mg, 1.0 mmol, 2.0 eq) was added under stirring. $Ph_2SnH_2$ (140 mg, 0.51mmol, 1.0 eq) was added dropwise, intense blistering started. A yellow-brownish oily precipitate formed in a clear mother liquor. The next day an additional equivalent $Ph_2SnH_2$ (140 mg, 0.51 mmol, 1.0 eq) was added, the mother liquor turned yellow and slightly blistering could be detected. The oily precipitate turned darker orange. After two weeks colorless crystals formed in the oily phase. Suitable for X-ray diffraction [$Ph_3SnSnPh_3$].

### [29] Reaction of $Ph_2SnH_2$ with *n*-BuLi and 12cr4 yielding hexadecaphenyl ocatstanna-1,8-diides $(Sn_8Ph_{16})Li_2$

In a 20 mL glass vial *n*-BuLi 1.6M (0.7 mL, 1.1 mmol, 2.2 eq) was dissolved in 10 mL DME under stirring. To that jellylike suspension $Ph_2SnH_2$ (140 mg, 0.51 mmol, 1.0 eq) with that 12cr4 (181mg, 1.0 mmol, 2.0 eq) was added dropwise, the jelly dissolved immediately and turned strongly yellow. After the complete addition stirring was stopped. The next day violet crystals formed suitable for X-ray diffraction.

$^1H$ NMR (300.22 MHz, $C_6D_6$): δ 7.86-7.84 (m, $H^{Ar}$), 7.75-7.12 (m, $H^{Ar}$,, overlay with solvent residual signal), 6.87-6.52 (m, $^1J_{H,119Sn}$ = 128.32 Hz, H; SnH), ppm. $^{119}Sn$ NMR (111.92 MHz, $C_6D_6$) δ -28.41 [$Ph_2SnMe_2$], -108.81 [$Ph_3SnLi$], -182.10 [$Ph_2HSnSnPh_2Li$] ($^1J_{Sn,H}$ = 128.32 Hz, SnH), -188.43 [$Ph_2HSnSnPh_2Li$] ppm.

### [30] Reaction of $Ph_2SnH_2$ and *n*-BuLi in diglyme to dodecaphenyl hexastanna-1,6-diides

In a 20 mL glass vial *n*-BuLi 1.6M (0.7 mL, 1.1 mmol, 2.2 eq) was dissolved in 10 mL diglyme. To that $Ph_2SnH_2$ (140mg, 0.51mmol, 1.0eq) was added dropwise under stirring. The reaction turned clear and dark yellow. Blistering could be detected. After a day, black crystals formed in an intense red mother liquor. Suitable for X-ray diffraction.

### [31] Reaction of $Ph_2SnH_2$ with $LiN(SiMe_3)_2$ in THF to $^{cy}[Ph_{10}Sn_6][Li{\cdot}(12cr4)_2]$

In a 20 mL glass vial $Ph_2SnH_2$ (275 mg, 1.0 mmol, 1.0 eq) was dissolved in 10 mL THF. To the colorless solution $LiN(SiMe_3)_2$ (167 mg, 1.0 mmol, 1.0 eq) was added. Strong blistering started immediately and the reaction turned light yellow. Red crystals formed in a yellow mother liquor,

which is removed by decantation, yielding light-red crystals. An UV/VIS spectrum could be observed. Crystals suitable for single crystal X-ray diffraction were obtained by recrystallisation.

$^{1}$H NMR (300.22 MHz, $C_6D_6$): δ 7.75-7.46 (m, 8 H; 8x $H^{Ar}$, overlay with solvent residual signal), 7.07-7.09 (m, 12 H; 12x $H^{Ar}$), 6.07 (s, $^{1}J_{H,119Sn}$ = 55.36 Hz, H; SnH) ppm. $^{119}$Sn NMR (111.92 MHz, $C_6D_6$): δ -182.10 (broad) [$Ph_2HSn$SnPh$_2$Li] ($^{1}J_{Sn,H}$ = 55.36 Hz), -188.25 [Ph$_2$HSn$SnPh_2$Li] ppm.

### [32] Reaction of $Ph_2SnH_2$ with $LiN(SiMe_3)_2$ in THF

In a 20 mL glass vial $LiN(SiMe_3)_2$ (43 mg, 0.25 mmol, 0.5 eq) was dissolved in 10 mL THF to a colorless clear solution. To that $Ph_2SnH_2$ (140 mg, 0.51 mmol, 1.0 eq) was added, the reaction turned light-yellow and foams slightly. The reaction was detected by NMR spectroscopy.

$^{1}$H NMR (300.22 MHz, $C_6D_6$): δ 7.76-7.75 (m, $H^{Ar}$), 7.40 (m, $H^{Ar}$), 6.91-6.62 (m, H; SnH) ppm. $^{119}$Sn NMR (111.92 MHz, $C_6D_6$): δ -181.83 [$Ph_2HSn$SnPh$_2$Li], -188.36 [Ph$_2$HSn$SnPh_2$Li] ppm.

### [33] Synthesis to didecaphenyl hexastanna-1,6-diides $(Sn_6Ph_{12})Li_2$ and red.polystannanes

In a 20 mL glass vial $Sn_6Ph_{12}$ (140 mg, 0.09 mmol, 1.0 eq) is dissolved in 10 mL diglyme to a colorless cloudy suspension. To that potassium (6.7 mg, 0.17 mmol, 2.0 eq) is added. The reaction turned slightly orange blistering could be detected. The next day red crystals **$(Sn_6Ph_{12})Li_2$** and black crystals **(red. polystannanes)** could be observed in an orange mother liquor. Suitable for X-ray diffraction.

### [34] Synthesis of poly (-$Ph_2Sn$-) and ($Ph_7Sn_3^-$)

In a 20 mL glass vial $Ph_2SnH_2$ (275 mg, 1 mmol, 1.0 eq) is dissolved in 10 mL dimethylether. To the light-yellow solution 12cr4 (356 mg, 2 mmol, 2.0 eq) and methyllithium (0.7 mL, 1.1 mmol, 1.1 eq) are added. Quickly the solution turned dark yellow. The next day small violet crystals formed in a clear red mother liquor. Three quarters of the supernatant are put in a new vial in the fridge. The next day long needlelike violet crystals formed **($Ph_7Sn_3^-$)**. Crystals are measured by X-ray diffraction.

### [35] Synthesis of poly (-$Ph_2Sn$-)

In a 20 mL glass vial $Ph_2SnH_2$ (297 mg, 1.1 mmol, 1.0 eq) is dissolved in 10 mL benzene. To the light-yellow solution 18cr6 (143 mg, 0.5 mmol, 0.5 eq) and potassium (21 mg, 0.5 mmol, 0.5 eq) were added. The reaction immediately turned dark yellow and blistering could be detected. The next day a black precipitate in a green mother liquor could be detected. Suitable for X-ray diffraction.

## Reactions of $Ph_2SnH_2$ with alkaline metals

### [36] Synthesis of $[Sn_8Ph_{16}][Li(12cr4)_2]_2$

Three pieces of Li were added to 100 mg $Ph_2SnH_2$ (0.36 mmol, 1.0 eq) with 130 mg 12cr4 (0.73 mmol, 2.0 eq) dissolved in 10 mL benzene. After ejection of the passivate layer, weakly blistering started, due to hydrogen evolution and the reaction turned slightly yellow. Three days later violet crystals in a yellow mother liquor formed. Suitable for X-ray analysis.

### [37] Synthesis of $[Sn_6Ph_{12}][Li(DME)_3]_2$

Three pieces of Li were added to 100 mg $Ph_2SnH_2$ (0.36 mmol, 1.0 eq) with 130 mg 12cr4 (0.73 mmol, 2.0 eq) dissolved in 10 mL DME. After ejection of the passivate layer, weakly blistering started, due to hydrogen evolution and the reaction turned slightly yellow. Three days later violet-greenish crystals in a red mother liquor formed. Suitable for X-ray analysis.

### [38] Synthesis of $[Sn_6Ph_{12}][Na(DME)_3]_2$ and $[Sn_4Ph_8][Na(15cr5)_2]_2$

12 mg Na (0.5 mmol, 0.5 eq) was added to 275 mg $Ph_2SnH_2$ (1 mmol, 1.0 eq) dissolved in 10 mL DME. Blistering started, due to hydrogen evolution and the reaction turned dark yellow. After 3h bubble formation stopped and the reaction was dark red. The next day red crystals formed ($[Sn_6Ph_{12}][Na(DME)_3]_2$). Half of the mother liquor was put in a new vial with 15cr5 (55 mg, 0.25 mmol, 0.25 eq) and in the fridge overnight. After three days orange crystals formed ($[Sn_4Ph_8][Na(15cr5)_2]_2$) suitable for X-Ray crystallography.

UV-VIS ($CH_3CN$) λ 404 nm

## [39] Synthesis of $[Sn_6Ph_{12}][K(DME)_3]_2$ and $[Sn_4Ph_8][K(18cr6)_2]_2$

20 mg K (0.5 mmol, 0.5 eq) was added to 275 mg $Ph_2SnH_2$ (1 mmol, 1.0 eq) dissolved in 10 mL DME. Blistering started, due to hydrogen evolution and the reaction turned dark yellow. After 3h bubble formation stopped and the reaction was dark red. The next day red crystals formed ($[Sn_6Ph_{12}][K(DME)_3]_2$). Half of the mother liquor was put in a new vial with 18cr6 (66 mg, 0.25 mmol, 0.25 eq) and in the fridge overnight. After three days orange crystals formed ($[Sn_4Ph_8][K(18cr6)_2]_2$) suitable for X-Ray crystallography.

## [40] Synthesis of $[Sn_6Ph_{12}][Rb(DME)_3]_2$ and $[Sn_4Ph_8][Rb(18cr6)_2]_2$

43 mg Rb (0.5 mmol, 0.5 eq) was added to 275 mg $Ph_2SnH_2$ (1 mmol, 1.0 eq) dissolved in 10 mL DME. Blistering started, due to hydrogen evolution and the reaction turned dark yellow. After 3h bubble formation stopped and the reaction was dark red. The next day red crystals formed ($[Sn_6Ph_{12}][Rb(DME)_3]_2$). Half of the mother liquor was put in a new vial with 18cr6 (66 mg, 0.25 mmol, 0.25 eq) and in the fridge overnight. After three days orange crystals formed ($[Sn_4Ph_8][Rb(18cr6)_2]_2$) suitable for X-Ray crystallography.

## [41] Synthesis of $[Sn_6Ph_{12}][Cs(DME)_3]_2$ and $[Sn_4Ph_8][Cs(18cr6)_2]_2$

62 mg Cs (0.5 mmol, 0.5 eq) was added to 275 mg $Ph_2SnH_2$ (1 mmol, 1.0 eq) dissolved in 10 mL DME. Blistering started, due to hydrogen evolution and the reaction turned dark yellow. After 3h bubble formation stopped and the reaction was dark red. The next day red crystals formed ($[Sn_6Ph_{12}][Cs(DME)_3]_2$). Half of the mother liquor was put in a new vial with 18cr6 (66 mg, 0.25 mmol, 0.25 eq) and in the fridge overnight. After three days orange crystals formed ($[Sn_4Ph_8][Cs(18cr6)_2]_2$) suitable for X-Ray crystallography.

## [42] Synthesis of $([Sn_6Ph_{12}][K(Diglyme)_3]_2)$

20mg K (0.5 mmol, 0.5 eq) was added to 275 mg $Ph_2SnH_2$ (1 mmol, 1.0 eq) dissolved in 10 mL diglyme. Blistering started, due to hydrogen evolution and the reaction turned dark yellow. After 3h bubble formation stopped and the reaction was dark red. The next day red-greenish crystals formed suitable for X-Ray crystallography.

UV-VIS ($CH_3CN$) λ 389, 452 nm

## [43] Synthesis of ($[Sn_6Ph_{12}][Rb(Diglyme)_3]_2$)

46 mg Rb(0.5 mmol, 0.5 eq) was added to 275 mg $Ph_2SnH_2$ (1 mmol, 1.0 eq) dissolved in 10 mL diglyme. Blistering started, due to hydrogen evolution and the reaction turned dark yellow. After 3h bubble formation stopped and the reaction was dark red. The next day red-greenish crystals formed suitable for X-Ray crystallography.

## [44] Synthesis of ($[Sn_6Ph_{12}][Cs(Diglyme)_3]_2$)

62 mg Cs(0.5 mmol, 0.5 eq) was added to 275 mg $Ph_2SnH_2$ (1 mmol, 1.0 eq) dissolved in 10 mL diglyme. Blistering started, due to hydrogen evolution and the reaction turned dark yellow. After 3h bubble formation stopped and the reaction was dark red. The next day red-greenish crystals formed suitable for X-Ray crystallography.

## [45] Synthesis of ($[Sn_8Ph_{16}][Na(Diglyme)_3]_2$)

10 mg Na (0.4 mmol, 0.4 eq) was added to 275 mg $Ph_2SnH_2$ (1 mmol, 1.0 eq) dissolved in 10 mL diglyme. Blistering started, due to hydrogen evolution and the reaction turned dark yellow. After 3h bubble formation stopped and the reaction was dark red. The next day red-greenish crystals formed suitable for X-Ray crystallography.

UV-VIS ($CH_3CN$) λ 349, 468, 557 nm

# 7 References


1. Mandal, S. K. & Roesky, H. W. Group 14 Hydrides with Low Valent Elements for Activation of Small Molecules. *Acc. Chem. Res.* **45**, 298–307 (2012).

2. Eichler, B. E. & Power, P. P. {2,6-trip2H3C6Sn(μ-H)}2 (Trip = C6H2-2,4,6-i-Pr3): Synthesis and structure of a divalent group 14 element hydride [5]. *J. Am. Chem. Soc.* **122**, 8785–8786 (2000).

3. Hadlington, T. J., Driess, M. & Jones, C. Low-valent group 14 element hydride chemistry: Towards catalysis. *Chem. Soc. Rev.* **47**, 4176–4197 (2018).

4. Al-Rafia, S. M. I., Malcolm, A. C., Liew, S. K., Ferguson, M. J. & Rivard, E. Stabilization of the Heavy Methylene Analogues, GeH 2 and SnH 2 , within the Coordination Sphere of a Transition Metal . *J. Am. Chem. Soc.* **133**, 777–779 (2011).

5. Abraham, M. Y. *et al.* Cleavage of carbene-stabilized disilicon. *J. Am. Chem. Soc.* **133**, 8874–8876 (2011).

6. Steller, B. G., Doler, B. & Fischer, R. C. Diaryltin dihydrides and aryltin trihydrides with intriguing stability. *Molecules* **25**, 1–16 (2020).

7. Kraus, C. A. & Greer, W. N. The preparation and properties of trimethylstannane. *J. Am. Chem. Soc.* **44**, 2629–2633 (1922).

8. Finholt, A. E., Bond, A. C., Wilzbach, K. E. & Schlesinger, H. I. The Preparation and Some Properties of Hydrides of Elements of the Fourth Group of the Periodic System and of their Organic Derivatives. *J. Am. Chem. Soc.* **69**, 2692–2696 (1947).

9. Zeppek, C., Pichler, J., Torvisco, A., Flock, M. & Uhlig, F. Aryltin chlorides and hydrides: Preparation, detailed NMR studies and DFT calculations. *J. Organomet. Chem.* **740**, 41–49 (2013).

10. Steller, B. Diorganotin dihydrides as Building Blocks for functionalised Oligomers and σ-conjugated Materials. (2017).

11. Davies, A. G. *Organotin Chemistry*. *Organotin Chemistry* (2004). doi:10.1002/3527601899.

12. Smith, N. D., Mancuso, J. & Lautens, M. Metal-catalyzed hydrostannations. *Chem. Rev.* **100**, 3257–3282 (2000).

13. Caseri, W. Polystannanes: Processible molecular metals with defined chemical structures. *Chem. Soc. Rev.* **45**, 5187–5199 (2016).

14. Reimann, W., Kuivila, H. G., Farah, D. & Apoussidis, T. Reactions of Organotin Hydrides with Lithium Diisopropylamide and Organolithiums: Reactivities of the Intermediates and of the Lithium Hydride Produced. *Organometallics* **6**, 557–565 (1987).

15. Podestá, J. C., Chopa, A. B., Giagante, N. N. & Zúñiga, A. E. Preparation and some reactions of neophyltin anions. *J. Organomet. Chem.* **494**, 5–10 (1995).

16. Schlosser, M. Polare Organometalle. in 3–8 (1973).

17. Reich, H. J. Role of organolithium aggregates and mixed aggregates in organolithium mechanisms. *Chem. Rev.* **113**, 7130–7178 (2013).

18. Tai, O., Hopson, R. & Williard, P. G. Aggregation and Solvation of n-Butyllithium. (2017) doi:10.1021/acs.orglett.7b01644.

19. Li, T. ', Rathman, ' & Schwindeman, J. A. Preparation, Properties, and Safe Handling of Commercial Organolithiums: Alkyllithiums, Lithium sec-Organoamides, and Lithium Alkoxides. (2014) doi:10.1021/op500161b.

20. Konig, K., Wilhelm, V. & Neumann, P. U B E R DIARYLZINN-DIHYDRIDE U N D Z l N N D l ARYLE MIT HOHEREN ARYLRESTEN ~ ). **215**, 12–18 (1964).

21. Davies, A. G. & Osei-Kissi, D. K. The formation of distannanes from tin hydrides. *J. Organomet. Chem.* **474**, 10–12 (1994).

22. Sindlinger, C. P., Stasch, A., Bettinger, H. F. & Wesemann, L. A nitrogen-base catalyzed generation of organotin(ii) hydride from an organotin trihydride under reductive

dihydrogen elimination. *Chem. Sci.* **6**, 4737–4751 (2015).

23. Neale, N. R. & Tilley, T. D. A new mechanism for metal-catalyzed stannane dehydrocoupling based on α-H-elimination in a hafnium hydrostannyl complex. *J. Am. Chem. Soc.* **124**, 3802–3803 (2002).

24. Choffat, F., Smith, P. & Caseri, W. Facile synthesis of linear poly(dibutylstannane). *J. Mater. Chem.* **15**, 1789–1792 (2005).

25. Bukalov, S. S., Leites, L. A., Lu, V. & Tilley, T. D. Order-disorder phase transition in poly(di-n-butylstannane) observed by UV-Vis and Raman spectroscopy. *Macromolecules* **35**, 1757–1761 (2002).

26. West, R. The polysilane high polymers. *J. Organomet. Chem.* **300**, 327–346 (1986).

27. Trummer, M. & Caseri, W. Diorganostannide dianions (R2Sn2-) as reaction intermediates revisited: In situ 119Sn NMR studies in liquid ammonia. *Organometallics* **29**, 3862–3867 (2010).

28. Wrackmeyer_NMR_B_Alkali_Sn.pdf.

29. Neumann, W. P. & Niermann, H. Darstellung Von Organozinn-Mono-, -Di- Und -Tri-Hydriden. *Eur. J. Inorg. Chem.* **653**, 164–172 (1962).

30. Brückner, R. *et al.* Ausgewählte Arbeitstechniken im Fortgeschrittenenpraktikum (in alphabetischer Reihenfolge). *Prakt. Präparative Org. Chemie - Org. Fortgeschrittenenpraktikum* 60–86 (2009).

31. Marsmann, H. C. & Uhlig, F. *Further Advances in Germanium, Tin and Lead NMR*. *PATAI'S Chemistry of Functional Groups* vol. 2 (2009).